

1 **Polar semi-volatile organic compounds in biomass burning emissions and their**  
2 **chemical transformations during aging in an oxidation flow reactor**

3 Deep Sengupta,<sup>1</sup> Vera Samburova,<sup>1</sup> Chiranjivi Bhattarai,<sup>1</sup> Adam C. Watts,<sup>1</sup> Hans Moosmüller,<sup>1</sup>  
4 Andrey Y. Khlystov<sup>1</sup>

5 <sup>1</sup>Desert Research Institute, 2215 Raggio Parkway, Reno, NV 89512, USA  
6  
7

8 *Correspondence to:* vera.samburova@dri.edu

9 **Abstract**

10 Semi-volatile organic compounds (SVOCs) emitted from open biomass-burning (BB) can  
11 contribute to chemical and physical properties of atmospheric aerosols and also may cause adverse  
12 health effects. The polar fraction of SVOCs is a prominent part of BB organic aerosols, and thus  
13 it is important to characterize the chemical composition and reactivity of this fraction. In this study,  
14 globally and regionally important representative fuels (Alaskan peat, Moscow peat, Pskov peat,  
15 Eucalyptus, Malaysian peat, and Malaysian agricultural peat) were burned under controlled  
16 conditions using the combustion chamber facility at the Desert Research Institute (DRI). Gas- and  
17 particulate-phase biomass-burning emissions were aged in an oxidation flow reactor (OFR) to  
18 mimic 5–7 days of atmospheric aging. Fresh and OFR-aged biomass-burning aerosols were  
19 collected on Teflon impregnated glass fiber filters (TIGF) in tandem with XAD resin media for  
20 organic compound (OC) speciation. The polar fraction extracted with dichloromethane and  
21 acetone was analyzed with gas chromatography mass spectrometry (GC-MS) for 84 polar organic  
22 compounds—including mono and dicarboxylic acids, methoxylated phenols, aromatic acids,  
23 anhydrosugars, resin acids, and sterols. For all these compounds, fuel-based emission factors (EFs)  
24 were calculated for fresh and OFR-aged samples. The carbon mass of the quantified polar  
25 compounds was found to constitute 5% to 7% of the total OC mass. High abundance of  
26 methoxyphenols (239 mg kg<sup>-1</sup> for Pskov peat; 22.6% of total GC-MS characterized mass) and resin  
27 acids (118 mg kg<sup>-1</sup> for Pskov peat; 14.5 % of total GC-MS characterized mass) was found in peat  
28 burning emissions (smoldering combustion). Concentration of some organic compounds (e.g.,  
29 tetracosanoic acid) with molecular weight (MW) above 350 g mol<sup>-1</sup> decreased after the OFR aging,  
30 while abundances of low MW compounds (e.g., hexanoic acid) increased. This indicated a  
31 significant extent of fragmentation reactions in the OFR. Methoxyphenols decreased after OFR  
32 aging, while a significant increase (3.7 to 8.6 times) in abundance of dicarboxylic acids emission

33 factors (EFs), especially maleic acid (10 to 60 times), was observed. EFs for fresh and ratios from  
34 fresh-to-aged BB samples reported in this study can be used to perform source apportionment and  
35 predict processes occurring during atmospheric transport.

36

37

38 **Keywords.** Biomass burning, organic aerosols, semi-volatile organic compounds (SVOCs), gas  
39 chromatography, mass spectrometry, polar organic compounds, oxidation flow reactor

40

## 41 **1 Introduction**

42 Biomass burning (BB), including both wildfires and prescribed burns, is a major source of  
43 carbonaceous aerosols in the atmosphere (Penner et al., 1991) and can contribute up to 75% of  
44 total atmospheric aerosol mass loading (Andreae et al., 2001; Park et al., 2007). These  
45 carbonaceous aerosols have significant impact on both regional and global radiative forcing  
46 (Ramanathan and Carmichael, 2008). BB emissions also can cause adverse health effects (Arbex  
47 et al., 2007; Regalado et al., 2006) because of the toxicological properties of particle-bound organic  
48 compounds (Chen et al., 2017; Pardo et al., 2020; Pavagadhi et al., 2013; Sigsgaard et al., 2015;  
49 Yang et al., 2010). Therefore, comprehensive, molecular-level characterization of BB emissions  
50 is essential for understanding health effects. Such molecular characterization of BB carbonaceous  
51 aerosols in the atmosphere, however, is challenging as these aerosols are composed of tens of  
52 thousands of compounds (Goldstein and Galbally, 2007).

53  
54 Simulation of natural fires in a laboratory environment using a BB chamber is one way to  
55 characterize the chemical composition of BB emissions (Yokelson et al., 2003). A number of  
56 studies characterizing the molecular composition of combustion emissions from fuels that  
57 represent different geographical regions have been completed: temperate conifers (Oros and  
58 Simoneit, 2001a), deciduous trees (Oros and Simoneit, 2001b), grasses (Oros et al., 2006), and  
59 peats (Samburova et al., 2016; Iinuma et al., 2007). Akagi et al. (2011) compiled fuel-based  
60 emission factors (EFs) from different fuels from throughout the world, including the peatlands of  
61 south Asia, and found that burning condition (flaming/smoldering) can influence the EFs of  
62 individual compounds. These data have been used for modeling work in predicting ozone-forming  
63 potential and other air quality impacts (Alvarado et al., 2015). Very few studies (e.g. (Samburova  
64 et al., 2016) have focused on peat emissions. However, the importance of investigating the  
65 combustion products from burning peat soils is multifaceted. Peat soils, comprised predominantly  
66 of partially decomposed organic material, represent one-fourth to one-third of global terrestrial  
67 carbon and are under threat of increased fire activity in both boreal and tropical latitudes, areas of  
68 widespread peatland occurrence (Turetsky et al., 2015). In addition to the implications of peat fires  
69 for the global C cycle, local impacts from burning of peatlands include public health and safety  
70 problems from degraded to air quality, as well as ecological changes due to altered surface  
71 hydrology in low-relief areas (Watts et al., 2015). Most source apportionment studies, however,

72 focused on characterization of fresh emissions and emissions of either particle-phase or gas-phase  
73 compounds.

74  
75 Significant changes in organic aerosol composition during atmospheric transport have been  
76 reported (Liu et al., 2017; Decker et al., 2019). These changes can impact local and regional air  
77 quality. Also, the role of Siberian peat burning in haze formation in the Korean peninsula (Jung et  
78 al., 2016) demonstrates the global impact of BB emissions and their atmospheric transport on  
79 regional air quality. Some laboratory studies found an increase in organic aerosol (OA) mass after  
80 photochemical aging (Ortega et al., 2013; Grieshop et al., 2009) while others observed a modest  
81 decrease (Bhattarai et al., 2018). There is still limited data on evolution of chemical composition  
82 of primary organic aerosols (POAs) during atmospheric aging. Some laboratory experiments  
83 demonstrated degradation of levoglucosan (Hennigan et al., 2010; Kessler et al., 2010) and  
84 oxidation of methoxyphenols in the gas phase (Yee et al., 2013) and aqueous phase (Net et al.,  
85 2011). These studies have more mechanistic implications than quantifying gross change after  
86 atmospheric oxidation. The reactivity of a pool of organic compounds in a complex mixture such  
87 as BB emissions is expected to be different mechanistically from individual compounds. This  
88 necessitates the need for studies of the evolution of organic compounds through bulk molecular  
89 level characterization of BB emissions. Recently, Fortenberry et al. (2018) characterized the  
90 chemical fingerprints of aged biomass-burning aerosols (leaf and hardwood of white oak) by  
91 performing oxidation in a potential aerosol mass oxidation flow reactor (PAM-OFR) and chemical  
92 analysis with a thermal desorption aerosol gas chromatograph aerosol mass spectrometer (TAG-  
93 AMS). In this study, denuders were used to remove gases and particles were introduced to OFR to  
94 evaluate only the changes in particulate BB emissions during OFR oxidation. However, the  
95 presence of both gas and particulate phase emissions in real BB emission and the partitioning of  
96 organic compounds in such a complex mixture can affect the reactivity inside the OFR and hence  
97 the fate of organic compounds during OFR aging. Bertrand et al. (2018) analyzed 71 organic  
98 compounds in BB emissions, sampled from a smog chamber, with high resolution time of flight  
99 mass spectrometry (HR-ToF-AMS). This study confirms that nitro-aromatic compounds are  
100 formed after OFR oxidation and that they can be used as SOA tracer. However, this study was  
101 focused on controlled wood (pellet) burning that is substantially different from wildland BB  
102 emissions. There is still a lack of understanding, however, regarding (1) major organic compounds

103 emitted from BB (especially from peat fuels), (2) their roles in atmospheric photochemical  
104 reactions, and (3) what compounds are responsible for light absorption of fresh and aged BB  
105 emissions.

106  
107 In this study, emissions from laboratory combustion of six globally important fuels (Alaskan peat,  
108 Moscow peat, Pskov peat, Eucalyptus, Malaysian peat, and Malaysian agricultural peat) were  
109 quantitatively analyzed for more than 250 individual organic species, and analyses of 84 polar  
110 organic species is presented in this paper. BB emissions generated in a combustion chamber were  
111 run through the OFR, mimicking approximately 5 to 7 days of atmospheric oxidation (Bhattarai et  
112 al., 2018), and the OFR output was analyzed to characterize aged BB emissions. BB emissions  
113 were collected on filter and XAD media to identify distribution of organic species between the gas  
114 and particle phases. For the polar fraction of collected organic compounds, we quantitatively  
115 analyzed a total of 84 compounds (methoxyphenol derivatives, dicarboxylic acids,  
116 monocarboxylic acids, aromatic acids, resin acids, and anhydrosugars). In the analyzed  
117 anhydrosugars, we paid special attention to levoglucosan, a derivative from cellulose (Simoneit et  
118 al., 1999), since levoglucosan has been widely used as a molecular tracer of BB emissions  
119 (Bonvalot et al., 2016; Maenhaut et al., 2016). Methoxyphenols also have been used in source  
120 apportionment studies (Schauer et al., 2001; Schmidl et al., 2008b, 2008a). These source  
121 apportionment studies, however, haven't combined such a wide range of different groups in a  
122 single investigation. Here we provide a detailed targeted chemical analysis of both gas- and  
123 particle-phase BB emissions from the combustion of individual biomass fuels from diverse  
124 geographical locations for both fresh and aged emissions. The goal of this research was to  
125 characterize EFs of gas- and particulate-phase individual polar organic species for six compound  
126 groups (methoxyphenols, dicarboxylic acids, monocarboxylic acids, aromatic acids,  
127 anhydrosugars, and resin acids) and to analyze their fate after the-OFR oxidation. In separate  
128 sections we discussed EFs obtained for fresh and OFR-aged BB samples. The fresh-to-aged ratio  
129 and top contributing organic species also are discussed. The comparison between fresh and OFR-  
130 aged BB emissions helps to understand the chemical evolution of BB plumes in the atmosphere  
131 and the obtained data can be used in future source apportionment and atmospheric modeling  
132 studies.

133

## 134 **2. Experiments**

### 135 **2.1 Fuel Description**

136 We selected six globally and regionally important BB fuels: Alaskan peat, Moscow peat, Pskov  
137 peat, Eucalyptus, Malaysian peat, and Malaysian agricultural peat. Five of these were peat fuels  
138 selected from different geographical locations, representing smoldering combustion and one  
139 (Eucalyptus) representing flaming combustion.

140 Peatland ecosystems, generally wetland or mesic ecosystems underlain by soils composed  
141 primarily of partially-decomposed biomass, contain mostly organic carbon and more than 20%  
142 mineral content, represent a vast terrestrial carbon pool, and are potentially vast sources of carbon  
143 flux to the atmosphere during wildfires that consume peat (Harden et al., 2000). Peatlands in high-  
144 latitude temperate and boreal regions are particularly vulnerable to increased fire-related carbon  
145 emissions resulting from climatic warming and increases in fire season length, while peatlands in  
146 low-latitude and tropical regions are threatened by factors such as deforestation for agriculture,  
147 urbanization, and drainage (Turetsky et al., 2015). We collected Alaskan peat samples from the  
148 upper 10 cm of soils within black spruce (*Picea mariana*) near crown forest (Chakrabarty et al.,  
149 2016). High-latitude and Eurasia samples here are from *Sphagnum*- and cotton grass- (*Eriophorum*  
150 spp.) dominated communities, collected from the Moscow (Odintsovo and Shatura districts) and  
151 Pskov regions of Russia. These regions are representative of oligotrophic peat bogs found widely  
152 across Siberia as well. Tropical peat in this study includes samples from two areas in Malaysian  
153 Borneo. One set of samples is from a *Dipterocarp*-dominated lowland forest with largely intact  
154 native land cover, while the second set is from a cleared agricultural area in the Kota Snamarahan  
155 region. All peat soils were extracted from the top 15 cm of the soil profile. The mass of the dry  
156 peat fuels varied from 70-100 g. The peat fuels were burned inside a metal pot which contains  
157 thermally insulating materials at its bottom and sides.

158

159 We selected Eucalyptus as a test fuel because of its prevalence across Australia and its important  
160 contribution to Australian wildland fires. In addition, economic losses and risk to life and property  
161 from fires in eucalypt forests are magnified by their proximity to both fire-prone ecosystems and  
162 large urban areas; often eucalypt-dominated stands form boundaries between these two land-use  
163 types. There are nearly 900 species of the genera *Eucalyptus*, *Corymba*, and *Angophora*, which

164 collectively comprise woody plants known as eucalypts. Native to Australia, eucalypt-dominated  
165 forests cover nearly 92 million ha (Hills, W.E.; Brown, 1978). In addition, the fast and hardy  
166 growth characteristics of eucalypts have made them popular in warm ecoregions of Europe as well  
167 as North and South America, where they readily escape cultivation and become established,  
168 dominant community types near urban areas where they were originally introduced. Because of  
169 their high oil content, rapid and dense growth, and vegetative structure, eucalypts are highly  
170 flammable and contribute to high fire risk in areas where they occur (Goodrick and Stanturf, 2012).  
171 The mass of the Eucalyptus fuel burned (i.e., ~650 g) was higher than that of peat fuels and this  
172 fuel was arranged similar to a common arrangement for campfires.

173

## 174 **2.2 Reagents and Materials**

175 We obtained high-performance liquid chromatography (HPLC) grade methanol and hexane from  
176 Fisher Scientific (Fair Lawn, NJ, USA) and used the following filters for sampling and further  
177 chemical analyzes: pre-fired (900 °C for 4 h) 47 mm diameter quartz-fiber filter (2500 Pallflex  
178 QAT-UP, Pall Life Sciences, Ann Arbor, MI, USA) for thermo-optical Elemental Carbon/Organic  
179 carbon (EC/OC) analysis, Teflon® filters (2500 Pallflex QAT-UP, Pall Life Science, Ann Arbor,  
180 MI, USA) for gravimetric particulate matter (PM) mass analysis, and Teflon-impregnated glass  
181 fiber (TIGF) 47 mm diameter filters (Fiber FilmT60A20, Pall Life Sciences, Ann Abor, MI, USA)  
182 for organic analysis. We purchased the following deuterated internal standards from Cambridge  
183 isotope laboratories (Tewksbury, MA, USA) and CDN isotopes (Pointe-Claire, Quebec, Canada):  
184 hexanoic-d11 acid, , succinic-d4 acid, decanoic-d19 acid, adipic-d10 acid, suberic-d12 acid,  
185 homovanillic-2,2-d2 acid, myristic-d27 acid, heptadecanoicd33 acid, oleic-9,10-d2 acid  
186 tetradecanedioic-d24 acid (CDN Isotopes, Quebec, Canada) and benzoic-d5 acid, levoglucosan-  
187 d7 and cholesterol-2,2,3,4,4,6-d6 (Cambridge Isotope Laboratories, Inc., MA, USA)

188

189

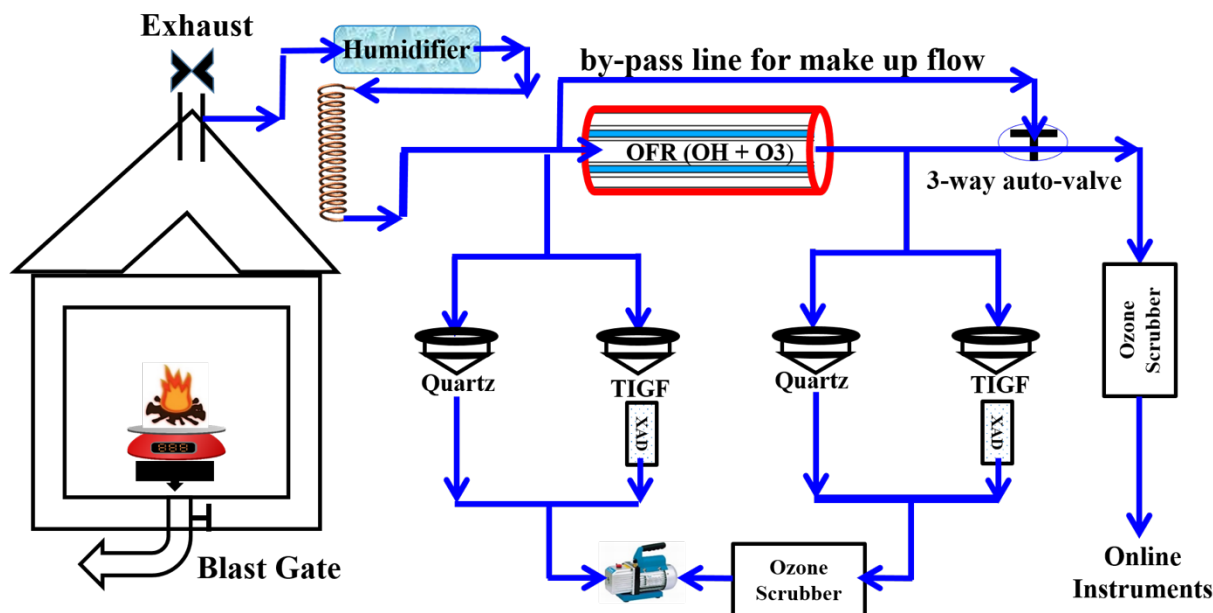
190

191

192

193

194 **2.3 Biomass Burning (BB) Experiments**



195  
196 **Figure 1.** Desert Research Institute (DRI) biomass burning (BB) facility with oxidative flow  
197 reactor (OFR) and flow setup.

198  
199 BB experiments were conducted using DRI’s BB facility for combustion of the selected fuels  
200 under controlled conditions. A close replicate of this facility was described previously (Tian et al.,  
201 2015), and a detailed description of the experimental setup was presented elsewhere (Bhattarai et  
202 al., 2018; Sengupta et al., 2018).

203  
204 We mixed laboratory-generated BB emissions with humidified zero air (Airgas Inc., Sparks, NV,  
205 USA) using 4 m long spiral copper tubing (12.7 mm OD). Before it was mixed with the BB  
206 emissions, the zero air was humidified by bubbling through Nano-pure water in a glass 500 mL  
207 volume impinger. The flow rate was controlled with a mass flow controller (810C-CE-RFQ-1821,  
208 Sierra Instruments, Monterey, CA, USA). An oxidation flow reactor (OFR) (Aerodyne Research  
209 Inc., Billerica, MA, USA) was used to mimic approximately seven days of equivalent atmospheric  
210 aging (Bhattarai et al., 2018). The OFR consisted of an alodine-coated aluminum cylinder (46 cm  
211 length and 22 cm diameter) with an internal volume of 13.3 L. Two sets of lamps emitted UV  
212 radiation at wavelengths of 185 and 254 nm (Atlantic Ultraviolet Corporation, Hauppauge, NY,  
213 USA) in the OFR to produce ozone and OH radicals (Li et al., 2015). UV irradiance in the OFR



214 was quantified using a photodiode detector with a wavelength range of 225 to 287 nm  
215 (TOCON\_C6; Sglux GmbH, Berlin, Germany). Ultra-high-purity nitrogen (Airgas Inc., Reno,  
216 NV, USA) was used to purge the UV lamp compartments to prevent the lamps from overheating.  
217 A probe that monitored relative humidity and temperature inside the OFR (from Aerodyne Inc.,  
218 MA, USA) was mounted toward the outlet side of the OFR. A detailed characterization of the  
219 OFR—such as particle loss, OH production rate, and time scales of various processes—can be  
220 found in Bhattarai et al. (2018).

221  
222 The duration of smoldering combustion experiments ranged from 69 to 255 min, whereas the  
223 average duration of flaming combustion experiments was 50 min. During all experiments, both  
224 fresh (directly from the chamber) and aged (oxidized in the OFR) emissions were continuously  
225 collected on a TIGF filter (for particle phase) followed by an XAD cartridge (for gas phase) for  
226 detailed chemical speciation. We used several online instruments to characterize gas- and particle-  
227 phase pollutants (see Fig. 1). Simultaneous collection of samples for thermal optical carbon  
228 analysis on quartz fiber filters (Pall-Gelman, 47 mm diameter, pre-heated) was conducted, but only  
229 for Eucalyptus and Malaysian peat. The online instruments alternated every 10 min between  
230 sampling fresh and aged emissions using a computer-controlled valve system. A description of all  
231 instruments and the detailed experimental set up can be found elsewhere (Bhattarai et al., 2018).

232  
233 We employed a bypass flow to keep the flow from the BB chamber and through the OFR constant  
234 when online instruments switched between sampling fresh and aged emissions. To protect online  
235 instruments from high ozone concentrations produced in the OFR, ozone scrubbers were installed  
236 in front of the instruments' inlets. The ozone scrubbers were loaded with charcoal followed by  
237 Carulite 200 catalyst (Carus Corp., Peru, IL, USA). There were no ozone scrubbers before the  
238 filter-XAD set up, which could cause further oxidation of organic compounds on filter surfaces  
239 during sampling. The reaction rates between organics and ozone, however, are orders of magnitude  
240 lower than OH oxidation reactions (Finlayson-Pitts and Pitts Jr, 1999). Therefore, we assumed that  
241 reactions with OH radicals were primarily responsible for changes in organic compounds  
242 associated with fresh gas and particulate emissions. We also acknowledge that the ozone-oxidation  
243 on the filters during the sampling can affect chemistry of the collected BB aerosols (section 3.4).

244

## 245 **2.4. Organic and Elemental Carbon (OC/EC) Analysis**

246 Emissions from the combustion of two fuels (Eucalyptus and Malaysian peat) were sampled with  
247 quartz-fiber filters, collected simultaneously with TIGF filters, for both fresh and aged BB aerosols  
248 (Supplementary Material, Fig. S1). Punches (area = 1.5 cm<sup>2</sup>) from these quartz filters were  
249 analyzed with a thermal-optical carbon analyzer (Atmoslytic Inc., Calabasas, CA, USA) following  
250 the IMPROVE protocol (Chow et al., 1993, 2004) for total organic carbon (OC<sub>Total</sub>) and elemental  
251 carbon (EC) mass.

252

## 253 **2.5 Analytical Methodology for GC-MS**

254 We extracted filter and XAD samples for GC/MS analysis (SI Table S1) yielding concentrations  
255 of 84 polar organic compounds. In addition, levoglucosan concentrations were determined using  
256 ion chromatography coupled with a pulsed amperometric detector (IC-PAD). Prior to the  
257 extraction, sampled TIGF filters and XAD-resin cartridges were spiked with deuterated internal  
258 standards (see “Reagents and Materials” section). The TIGF filters and XAD cartridges were  
259 extracted separately with an accelerated solvent extractor (Dionex ASE-300, Sunnyvale, CA,  
260 USA) at the following conditions: 80° C temperature, 250 mL extraction volume, and subsequent  
261 extraction with dichloromethane and acetone. The XAD and filters were treated separately to  
262 evaluate the speciation of gas- and particle-phase semi-volatile polar compounds. The extracts  
263 were concentrated with a rotary evaporator (Buchi-R124, Switzerland), filtered using 0.2 µm pore  
264 size syringe filters (Thermo Scientific, Redwood, TN, USA), and pre-concentrated with nitrogen  
265 to a volume of 4 mL. Then we split the extracts into two fractions. One fraction was transferred to  
266 2.0 mL volume deactivated glass maximum recovery vials (Waters Corporation, Milford, MA,  
267 USA), pre-concentrated to 50 µL volume under ultra-high-purity nitrogen (Airgas, Reno, NV,  
268 USA), and derivatized with N,O-bis-(trimethylsilyl) trifluoroacetamide (BSTFA with 1% of  
269 trimethylchlorosilane; Thermo-Scientific, Bellefonte, PA, USA) and pyridine as described  
270 elsewhere (Rinehart et al., 2006). Derivatized samples were analyzed by electron impact ionization  
271 using a Varian CP-3400 gas chromatograph with a CP-8400 auto-sampler and interfaced to a  
272 Varian 4000 ion trap mass spectrometer (Varian Inc. Palo Alto, CA, USA). The second fraction of  
273 non-derivatized extracts was kept for further analysis of non-polar organic species (e.g., alkanes  
274 and PAHs), and those results will be presented in future publications.

275 Since, we have not performed any replicate burning experiments in this study, we used uncertainty  
276 values from our previous work (Yatavelli et al., 2017) as follows. We took mean ( $\mu_c$ ) and standard  
277 deviation ( $\sigma_c$ ) values for all 84 compounds from Alaskan peat (3 replicates) and Cheatgrass (3  
278 replicates) combustion and calculated fractional uncertainties ( $f_c$ ) using equation 1.

$$279 \quad f_c = \frac{\mu_c}{\sigma_c} \quad \text{Eq. 1}$$

280 These fractional uncertainty values are multiplied by the emission factors for each compound (both  
281 fresh and aged) from the current study to obtain individual uncertainties or standard deviation (SD)  
282 values as demonstrated in equation 2.

$$283 \quad SD_c = f_c \times EF_c \quad \text{Eq. 2}$$

284 The group uncertainties for each different subclass were computed from individual uncertainties  
285 by applying standard propagation of error method (root sum of squares).

286 Considering the different nature of combustion, the fractional uncertainties derived from Alaskan  
287 peat combustion were applied to emissions from all peat fuels and the uncertainties obtained from  
288 cheatgrass combustion were applied to emissions from Eucalyptus combustion.

289

## 290 **2.6. Levoglucosan Analysis**

291 Portions of quartz filters collected for OC/EC analysis also were used for quantitative analysis of  
292 levoglucosan concentration with IC-PAD. Prior to the analysis, quartz filters were extracted with  
293 15 ml of deionized water (18.2 M $\Omega$ ), sonicated for one hour, and refrigerated overnight. The  
294 column temperature for IC was 25° C. Analytes along with a mixture of two eluents (48%  
295 hydroxide solution and 52% deionized water) were passed through the IC column with a 0.4 ml  
296 min<sup>-1</sup> eluent flow rate and detected using an electrochemical detector. See Chow and Watson  
297 (2017) for details. Uncertainties or standard deviations associated with levoglucosan results  
298 indicate only analytical uncertainties of the IC-PAD method.

299

## 300 **3. Results and Discussion**

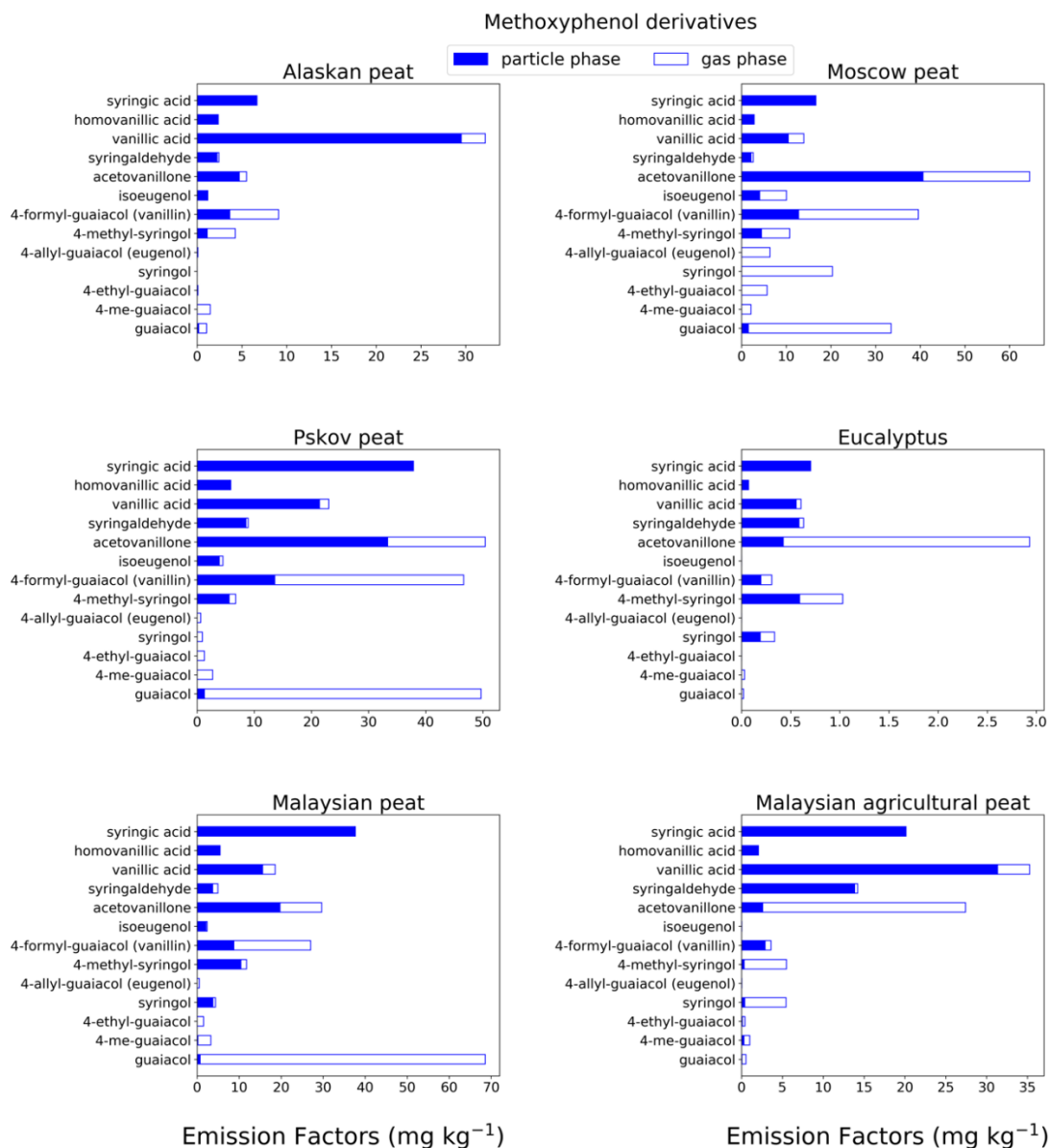
301

### 302 **3.1. Gas- and Particulate-Phase Emission Factors**

303 Organic compounds (84 in total) in fresh emissions identified and quantified in this study were  
304 assigned to six major groups (Table S1): methoxyphenol derivatives, dicarboxylic acids, mono-

305 carboxylic acids, aromatic acids, resin acids, and levoglucosan. First, we report individual  
306 emission factors (EF) belonging to a particular group calculated by summation of gas- and particle-  
307 phase EFs of individual compounds. Relative abundance of these compounds is reported next  
308 followed by a comparison of the contributions of each group ( $EF_{\text{group}}$ ) among fuels and a  
309 comparison with previously reported results.

310



312

313 Figure 2a. EFs for methoxyphenols in both particulate phase (solid bars, filter samples) and gas-  
 314 phase (open bars, XAD samples) from fresh biomass burning emissions for six different fuel types.  
 315 We did not burn fuels in replicates, and standard deviations (SD) were calculated based on replicate  
 316 analysis of emissions from similar fuels (with identical experimental conditions) during our  
 317 previous combustion campaigns (Yatavelli et al., 2017) where SD ranged between 9.7 and 22%  
 318 for methoxyphenol derivatives.

319 Methoxyphenols are key compounds in BB smoke since they constitute from 20 to 40% of total  
320 identified organic aerosol mass (Hawthorne et al., 1989; Yee et al., 2013). For this reason, these  
321 compounds are considered potential markers for wood combustion (Schauer et al., 2001) and have  
322 been used as probable biomarkers to determine human exposure to BB emissions (Simpson and  
323 Naeher, 2010; Dills et al., 2006). Our analysis of 13 methoxyphenols (Fig. 2a, Table S1) showed  
324 that guaiacol (MW = 124 g mol<sup>-1</sup>) was the major contributor to EFs of the measured  
325 methoxyphenols in Moscow peat (33.5±3.3 mg kg<sup>-1</sup>), Pskov peat (49.7±4.8 mg kg<sup>-1</sup>), and  
326 Malaysian peat (68.6±6.7 mg kg<sup>-1</sup>). Syringol, another methoxyphenol commonly found in BB  
327 emissions (Schauer et al., 2001), had the highest EF for Moscow Peat fresh emissions (20.4±2.7  
328 mg kg<sup>-1</sup>), while for the other fuels, the EF was much lower (0–5.5 mg kg<sup>-1</sup>). EFs for syringic acids  
329 (MW = 198 g mol<sup>-1</sup>) were in the range of 0.06–37.9 mg kg<sup>-1</sup> for all fresh emissions. Syringols are  
330 generally not formed during pyrolysis of coniferous lignin, but during pyrolysis of deciduous  
331 lignin, where both guaiacols and syringols are formed (Mazzoleni et al., 2007). Presence of both  
332 guaiacol and syringol moieties in fresh emissions indicates that the part of the plant material that  
333 was responsible for peat formation was probably from deciduous trees, and this signature of  
334 deciduous trees from peat burning emission is irrespective of geographical origin of those peats  
335 (also shown by Schauer et al., 2001). Acetovanillone, vanillin, and vanillic acid also were observed  
336 in fresh emissions with high abundance (5–50 mg kg<sup>-1</sup>). For example, vanillin is an abundant  
337 methoxyphenol in the fresh emissions from Pskov peat (46.7±5.4 mg kg<sup>-1</sup>) which contributed 4.4%  
338 of the total mass of the 84 analyzed compounds.

339

340 Low MW methoxyphenols (e.g., guaiacol) are expected to be found in the gas phase (Yatavelli et  
341 al., 2017), in close agreement with our results. For example, guaiacol and substituted guaiacols  
342 were mostly present in gas phase (82–100%) for emissions from the combustion of different fuels  
343 (Fig. 2a, Table S1). With the addition of more oxygenated functional groups to a molecule, and  
344 thus with MW increase, the equilibrium gas-particle partitioning of the compound tends to shift  
345 toward the particulate phase, which also was confirmed by our results (e.g., for acetovanillone, a  
346 keto form of lignin derivative, from Malaysian peat combustion, 33.5% of its mass was found in  
347 gas phase; for more oxygenated syringic acid, 99% of its mass was found in particulate phase  
348 emissions from the same fuel).

349 The highest methoxyphenol  $EF_{\text{group}}$  from combustion of all fuels was observed in the fresh Pskov  
350 peat (Fig. 3a) emissions ( $239 \pm 11 \text{ mg kg}^{-1}$ ). For Moscow peat, which was sampled close to the  
351 geographical region of Pskov peat, the  $EF_{\text{group}}$  of methoxyphenols was  $229 \pm 10 \text{ mg kg}^{-1}$  (Fig. 3a),  
352 very similar to that for Pskov peat. The methoxyphenol  $EF_{\text{group}}$  for peat samples were in the range  
353 of 66 to  $239 \text{ mg kg}^{-1}$  (Fig. 3a) for our 13 analyzed compounds. A previous study analyzed for 30  
354 different compounds (Schauer et al., 2001) and consequently found a larger value  $EF_{\text{group}}$  of up to  
355  $1330 \text{ mg kg}^{-1}$ , at least partially a result of the larger number of compounds analyzed. Formation  
356 of methoxyphenols during biomass combustion is mainly because of pyrolysis of lignin (e.g.,  
357 Simonelt et al., 1993). Lignin, an essential biopolymer of wood tissue, is primarily derived from  
358 three aromatic alcohols: p-coumaryl, coniferyl, and sinapyl alcohols (Hedges and Ertel, 1982).  
359 Lignins of hardwoods (angiosperms) are enriched with products from sinapyl alcohol; softwoods  
360 (gymnosperms) instead have a high proportion of products from coniferyl alcohol with a minor  
361 contribution from sinapyl alcohol; grasses have mainly products from p-coumaryl alcohol. The  
362 relative proportions of these bio-monomers vary considerably among the major plant classes  
363 (Sarkanen and Ludwig, 1971), reflected in our total emission factors estimate for 13  
364 methoxyphenols.

365

366

367

368

369

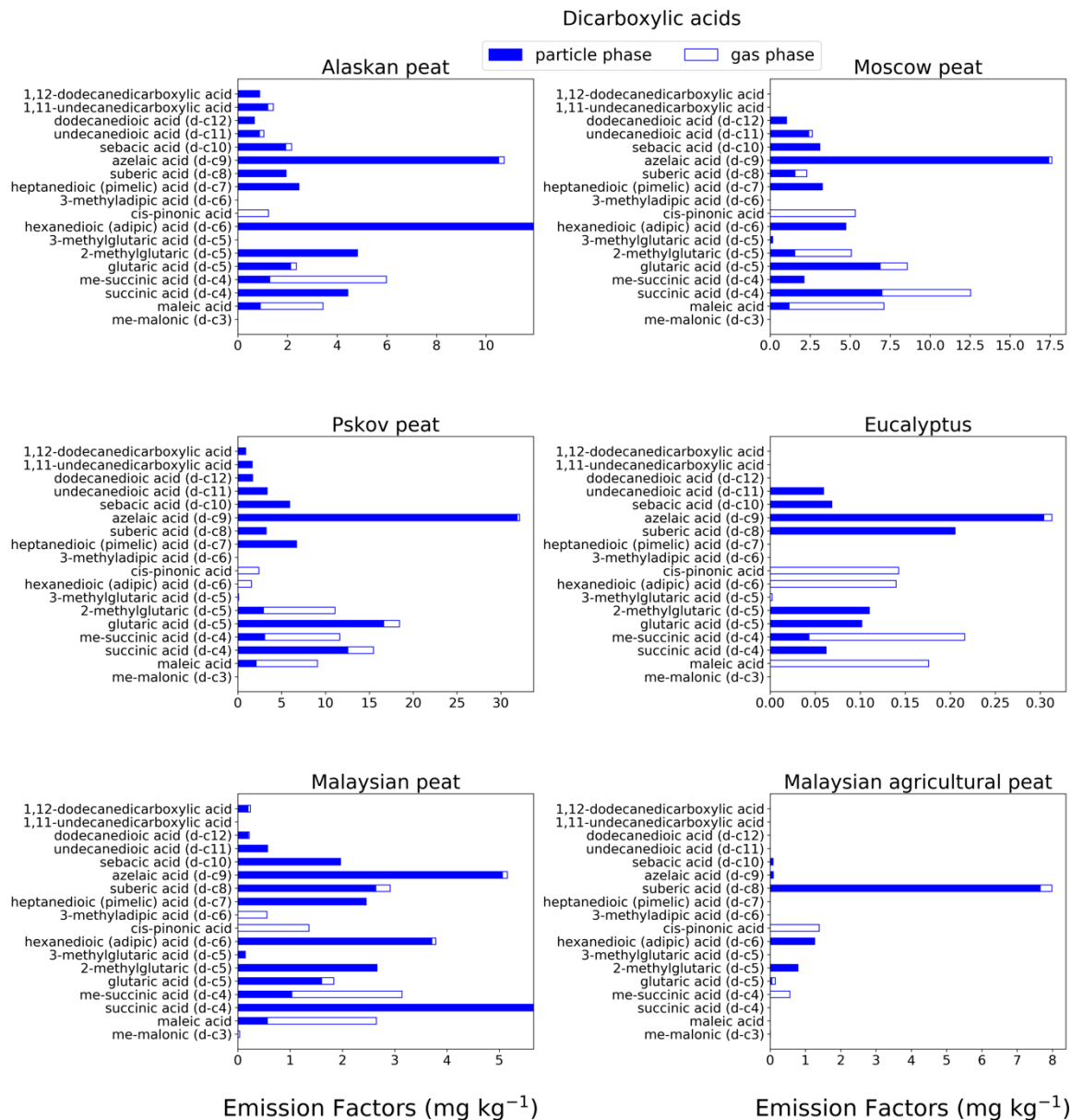
370

371

372

373

374

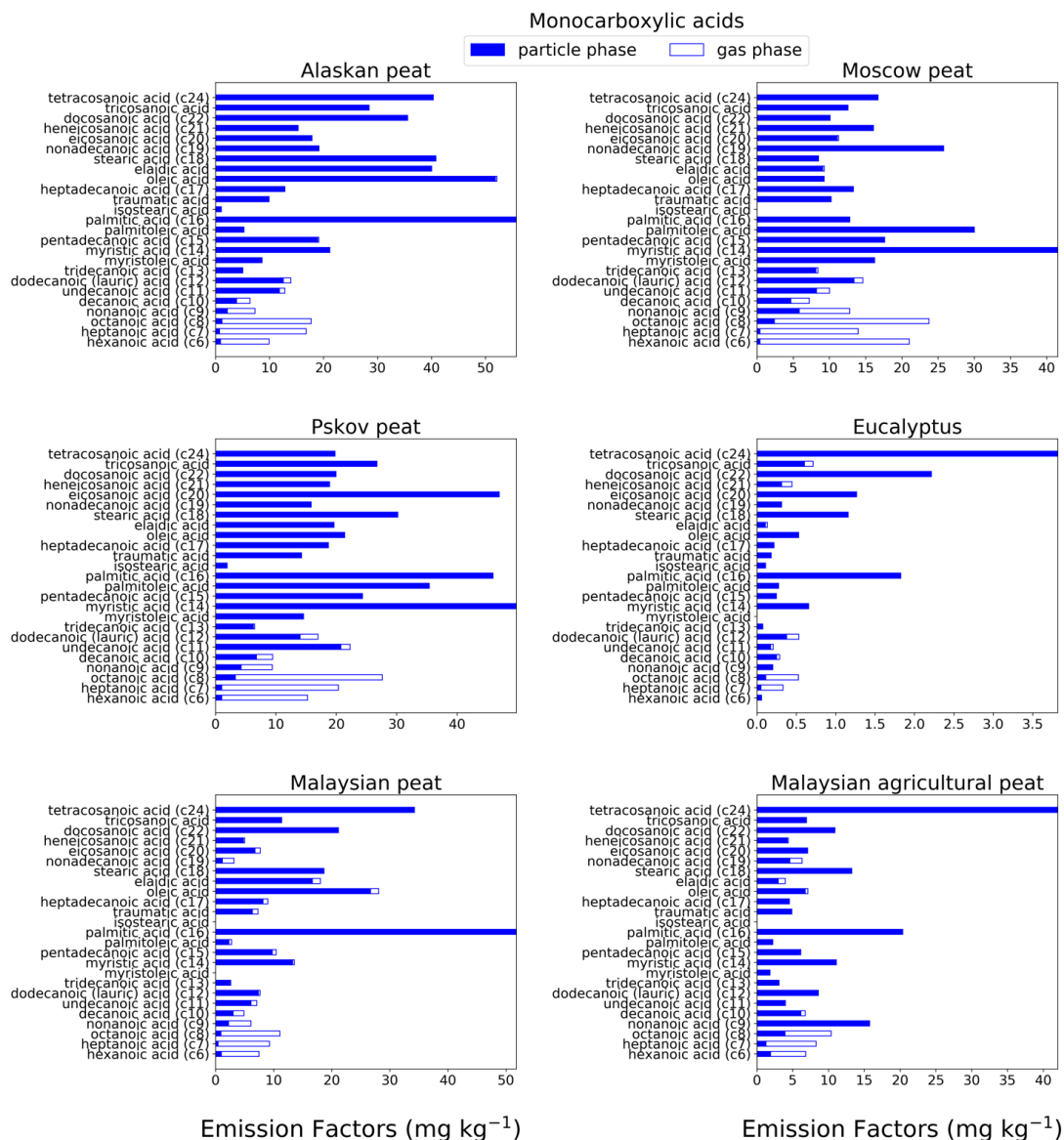


376

377 Figure 2b. EFs for dicarboxylic acids in both particulate phase (solid bars, filter samples) and  
 378 gas phase (open bars, XAD samples) from fresh biomass-burning emissions for six different fuel types.  
 379 We did not burn fuels in replicates, and standard deviations (SD) were calculated based on replicate  
 380 analysis of emissions from similar fuels (with identical experimental conditions) during our  
 381 previous combustion campaigns (Yatavelli et al., 2017) where SD ranged between 10 and 17% for  
 382 dicarboxylic acids.



383 Dicarboxylic acids play a significant role in the atmospheric organic aerosols budget (Samburova  
384 et al., 2013; Yatavelli et al., 2017) via secondary organic aerosol formation that either changes  
385 radiative forcing directly, or indirectly by acting as cloud condensation nuclei (Kawamura and  
386 Bikkina, 2016). The  $EF_{\text{group}}$  for dicarboxylic acids (Fig. 3b) varied among the fuels with the highest  
387  $EF$  for fresh Pskov peat samples ( $123 \pm 10 \text{ mg kg}^{-1}$ ) and with the lowest for Eucalyptus ( $1.5 \pm 0.1$   
388  $\text{mg kg}^{-1}$ ). This range in  $EF$ s can be attributed to difference in fuel type and burning conditions  
389 (smoldering vs. flaming). We also observed, however, a difference in the  $EF_{\text{group}}$  of dicarboxylic  
390 acid between two tropical peats from the same geographical area (Malaysian peat:  $EF = 35.33 \pm 2.9$   
391  $\text{mg kg}^{-1}$  and Malaysian agricultural peat:  $12.29 \pm 1.02 \text{ mg kg}^{-1}$ ). The highest  $EF$  for individual  
392 dicarboxylic acids was observed for azelaic acid. For example, for Pskov peat the  $EF$  was  $32.1 \pm 4.1$   
393  $\text{mg kg}^{-1}$ ; and for Moscow peat it, was  $17.6 \pm 2.6 \text{ mg kg}^{-1}$ . Azelaic acids were mostly found in the  
394 particulate phase (Fig. 2b, Table S1) and their relative abundances in the gas phase varied between  
395 0.77% (for Pskov peat) and 2.85% (for Eucalyptus). Maleic acid was mostly found in the gas phase  
396 (73%–83%), since it is a lower MW compound ( $MW = 116.0 \text{ g mol}^{-1}$ ) compared to azelaic  
397 ( $MW = 188.22 \text{ g mol}^{-1}$ ) and adipic ( $146.14 \text{ g mol}^{-1}$ ) acids. Succinic and methyl-succinic acids are  
398 found in both gas and particulate phases (Table S1), and their abundance in the particulate phase  
399 was 19–59% and 53–100%, respectively. For Malaysian peat BB emissions, succinic acid was  
400 present only in the particulate phase. A distinguishable increase in dicarboxylic acid mass  
401 concentrations was observed for ambient aerosols followed by a biomass burning event (Cao et  
402 al., 2017) compared to normal ambient concentrations. The formation of saturated dicarboxylic  
403 acids (e.g., succinic acid) and unsaturated dicarboxylic acids (e.g., maleic acid) also was reported  
404 for ambient aerosols collected near a biomass-burning event (Graham et al., 2002; Kundu et al.,  
405 2010; Zhu et al., 2018) and in ice core records historically affected by biomass burning (Müller-  
406 Tautges et al., 2016).



408  
 409 Figure 2c. EFs for monocarboxylic acids in both particulate phase (solid bars, filter samples) and  
 410 gas-phase (open bars, XAD samples) from fresh biomass burning emissions for six different fuel  
 411 types. We did not burn fuels in replicates and standard deviations (SD) were calculated based on  
 412 replicate analysis of emissions from similar fuels (with identical experimental conditions) during  
 413 our previous combustion campaigns (Yatavelli et al., 2017) where SD ranged between 9.4 and  
 414 12% for monocarboxylic acids.  
 415

416 Monocarboxylic acids can constitute up to 30–40% of total identified organic aerosol mass from  
417 BB emissions (Oros et al., 2006). In our study, we characterized the range from C<sub>6</sub>–C<sub>24</sub>, where  
418 some unsaturated monocarboxylic acids (e.g., oleic acid) also are included. For Alaskan and  
419 Malaysian peat fresh emissions (Fig. 2c), the highest EF (gas + particle) among all analysed  
420 monocarboxylic acids was for hexadecanoic acid (C<sub>16</sub>) with EFs of 55.7±6.6 mg kg<sup>-1</sup> and 51.8±6.2  
421 mg kg<sup>-1</sup>, respectively. The dominance of hexadecanoic acid among other monocarboxylic acids in  
422 combustion emissions also was observed in ambient measurements during biomass-burning events  
423 in southeast Asia (Fang et al., 1999). For Moscow (41.5±6.5 mg kg<sup>-1</sup>) and Pskov (49.8±7.8 mg kg<sup>-1</sup>)  
424 peats, tetradecanoic acid (C<sub>14</sub>) had the highest EFs in fresh samples (Fig. 2c). For Eucalyptus  
425 and Malaysian agricultural peat fresh samples, the largest contributor to monocarboxylic acids was  
426 tetracosanoic acid (C<sub>24</sub>) (Fig. 2c) with EFs of 3.81±0.5 mg kg<sup>-1</sup> and 42.0±5.1 mg kg<sup>-1</sup>, respectively.  
427 As we expected, low MW monocarboxylic acids like hexanoic acid (MW=116 g mol<sup>-1</sup>) was mostly  
428 present in the gas phase, and the gas phase mass fraction varied between 72% (for Malaysian  
429 agricultural peat) and 98% (for Moscow peat). Similar trends were observed for other low MW  
430 monocarboxylic acids. For example, the relative abundance of octanoic acid (C<sub>8</sub>) in the gas phase  
431 was 93.4% for Alaskan peat. High MW monocarboxylic acids (C<sub>16</sub>>) abundance in the gas phase  
432 was < 2% for all analyzed fuels.

433  
434 Carbon preference index (CPI) is generally used for source apportionment of organic aerosols  
435 (Fang et al., 1999). We also computed the carbon preference index for monocarboxylic acids from  
436 all analyzed fuel combustion emissions by taking even carbon number over odd carbon number  
437 ratio on EFs of monocarboxylic acids ranges from C<sub>6</sub> to C<sub>24</sub> (Fig. S1). For fresh emission samples,  
438 the CPI values ranged from 1.28 (for Moscow peat) to 4.53 (for Eucalyptus). The CPI values are  
439 higher for fresh emissions of tropical peats (for example, 2.78 for Malaysian peat) than for  
440 emissions from peats from high latitudes (for example, 1.74 for Pskov peat). An average CPI index  
441 of 3.7 for monocarboxylic acids was reported for combustion emissions from sedimentary bogs  
442 (Freimuth et al., 2019), in the range of our reported values (CPI: 1.3–4.5).

443  
444 The sums of the EFs for 25 monocarboxylic acids are shown in Fig. 3c. The EF<sub>group</sub> was in the  
445 range of 5 and 515 mg kg<sup>-1</sup> for all fuels. This range is comparable to the EF<sub>group</sub> reported previously

446 for grass (tundra, cotton, Pampas and ryegrass) combustion (32–250 mg kg<sup>-1</sup>) (Oros et al., 2006).  
447 Overall, the trend of low EFs associated with flaming combustion of Eucalyptus (16±0.7 mg kg<sup>-1</sup>)  
448 compared to smoldering peat combustion is also evident for this compound category. Combustion  
449 of peat fuels from tropical regions (e.g., Malaysian agricultural peat) resulted in monocarboxylic  
450 acids EFs of 212±9.6 mg kg<sup>-1</sup> compared to higher EFs from Alaskan peat combustion (505±23 mg  
451 kg<sup>-1</sup>). The origin of monocarboxylic acid is mostly plant wax and oils (Simoneit, 2002). The  
452 relative proportion of plant wax and oils can vary widely among vegetation taxa and also their  
453 concentrations in peat depend on biogeochemical processes involved in peat formation. The  
454 differences in relative abundance of waxes and plant oils in living vegetation and the differences  
455 between biogeochemical processes involved in peat formation for arctic and tropical regions may  
456 be responsible for diverse EFs for monocarboxylic acids.

457

458

459

460

461

462

463

464

465

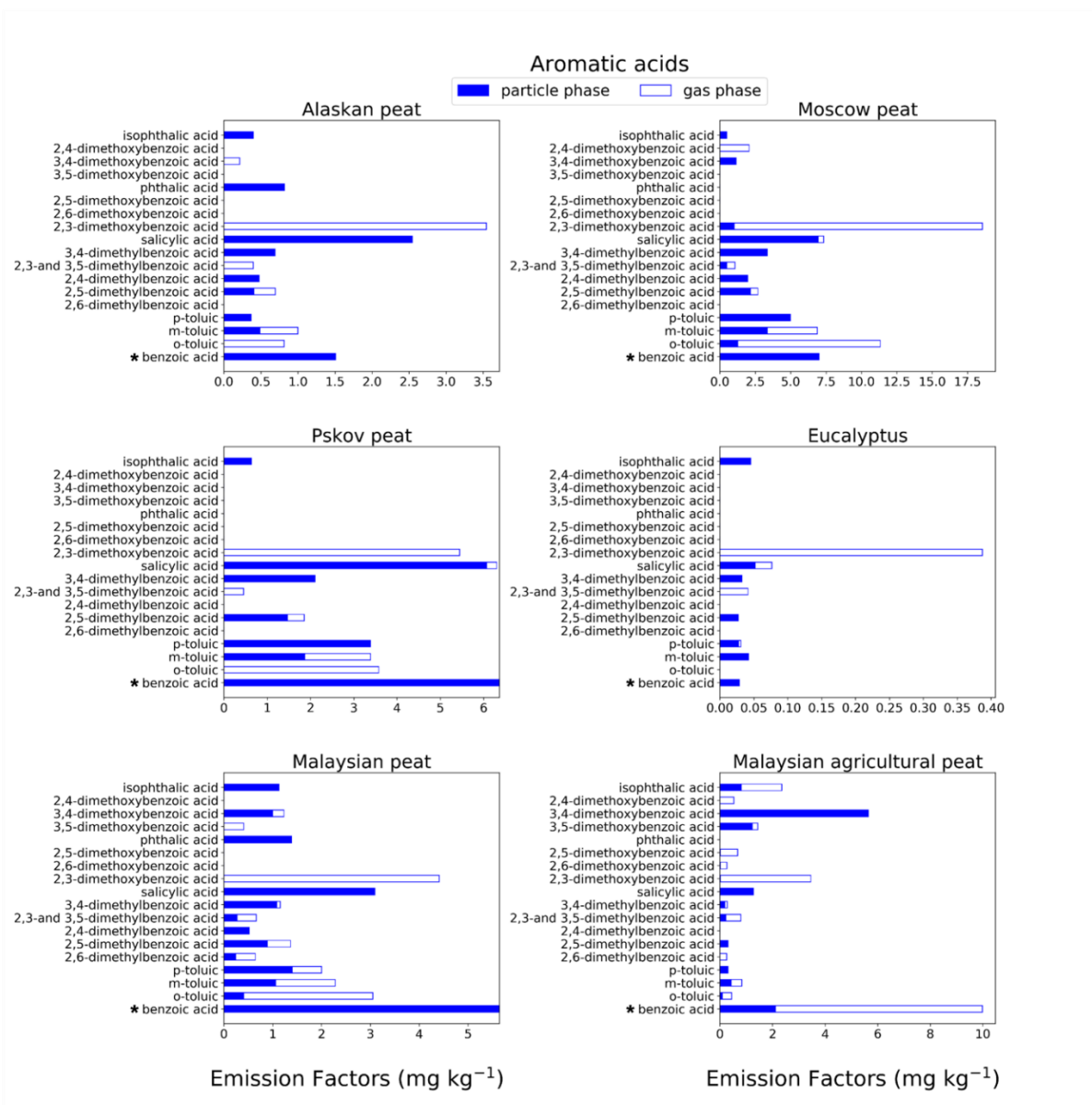
466

467

468

469

470



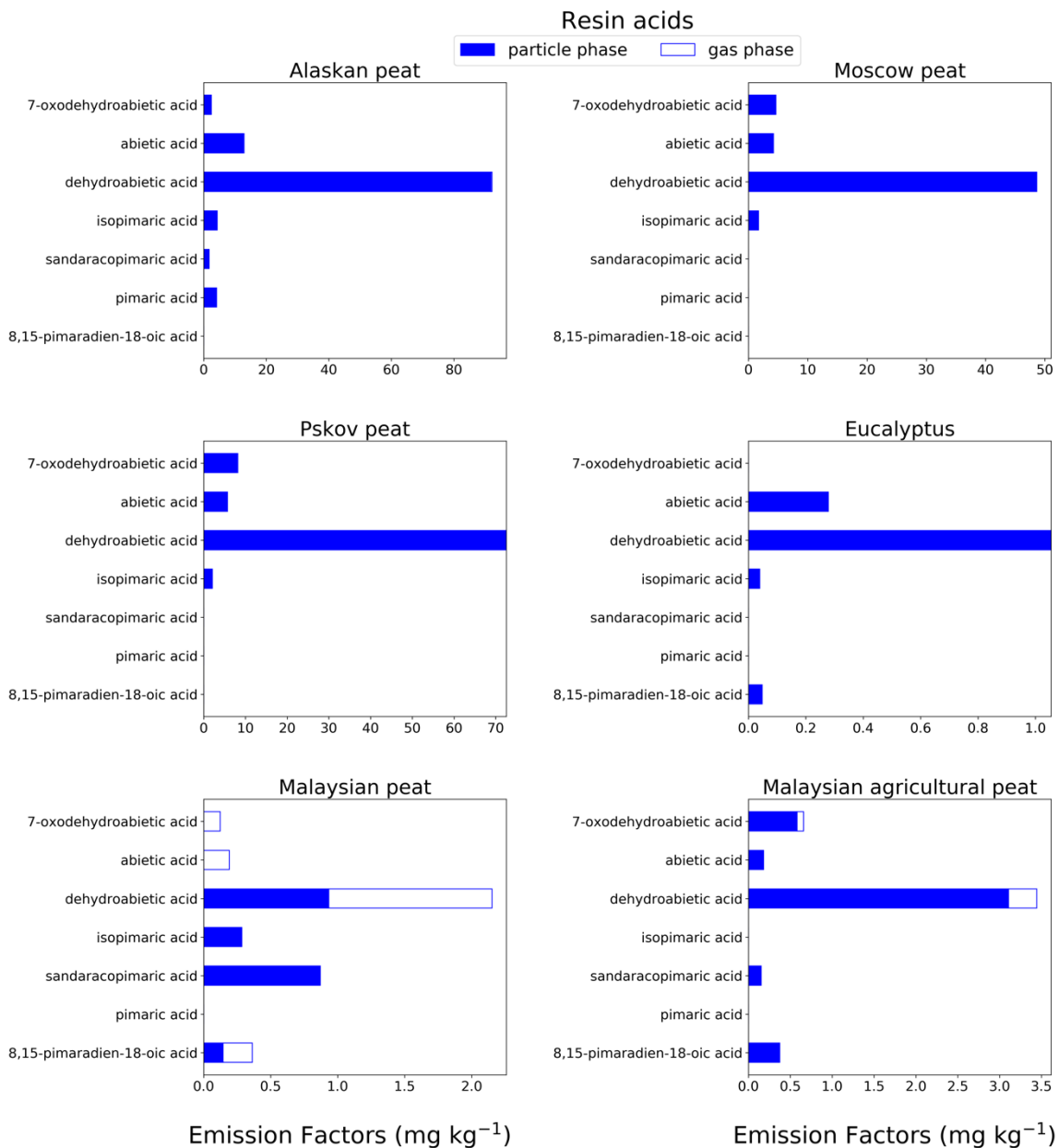
472  
 473 Figure 2d. EFs for aromatic acids in both particulate phase (solid bars, filter samples) and gas-  
 474 phase (open bars, XAD samples) from fresh biomass burning emissions for six different fuel types.  
 475 We did not burn fuels in replicates, and SD were calculated based on replicate analysis of  
 476 emissions from similar fuels (with identical experimental conditions) during our previous  
 477 combustion campaigns (Yatavelli et al., 2017) where SD ranged between 9.5 and 15% for aromatic  
 478 acids; \*Benzoic acid was found in high concentrations in the XAD blanks that introduced a  
 479 substantial uncertainty to quantification of this compound.

480 Aromatic acids from BB emissions can contribute up to 20–35 % of total identified organic mass  
481 (Wan et al., 2019). In our study, the aromatic acids (e.g., p-hydroxy benzoic acid), excluded  
482 methoxyphenol derivatives and resin acids. For most of the fuels, low MW aromatic acids (MW  
483  $<150 \text{ g mol}^{-1}$ ) (e.g., benzoic acid, o-/m-/p-toluic acids) contributed more (almost 40% of total  
484 aromatic acid emissions) toward total fresh emissions, compared to high MW aromatic acids (MW  
485  $>150 \text{ g mol}^{-1}$ ). For example, the benzoic acid EF for Malaysian agricultural peat fresh emission  
486 (Fig. 2d) is  $9.98 \pm 1 \text{ mg kg}^{-1}$ , and the EF for the same benzoic acid is  $6.36 \pm 0.6 \text{ mg kg}^{-1}$  for Pskov  
487 peat (Fig. 2d). Although, o-toluic and p-toluic acids are found in gas phase with 50%–100%  
488 abundance in Alaskan and Moscow peat, benzoic acid is found only in particulate phase. Benzoic  
489 acid was found in high concentrations in the XAD blanks that introduced a substantial uncertainty  
490 to quantification of this compound. One of the most abundant aromatic acids in fresh peat  
491 emissions was 2,3-dimethoxy benzoic acid. For example, for Moscow peat the EF was  $18.6 \pm 4.7$   
492  $\text{mg kg}^{-1}$ . The acid was mostly found in gas phase (91%–100%) for all fuels (Fig. 2d, Table S1).  
493 2,3-dimethoxy benzoic acid is potentially derived from combustion of lignin moieties of biomass,  
494 and the emission of this compound is more than an order of magnitude lower in emissions from  
495 flaming combustion samples ( $\text{EF} = 0.38 \pm 0.09 \text{ mg kg}^{-1}$ ) than in emissions from smoldering  
496 combustion emissions ( $\text{EF} = 5.44 \pm 1.36 \text{ mg kg}^{-1}$ ). Emissions of 3,4 dimethoxy benzoic acid were  
497 only observed for peats from tropical regions ( $\text{EF} = 5.64 \pm 0.8 \text{ mg kg}^{-1}$ ) with 80–100% abundance in  
498 particulate phase. This compound can be used for source apportionment of aerosols emitted from  
499 burning of tropical peat and also can potentially help to distinguish between emissions from  
500 tropical and high latitude peatland fires.

501  
502 The  $\text{EF}_{\text{group}}$  for aromatic acids in fresh combustion emissions from eucalyptus fuel is extremely  
503 low ( $0.71 \pm 0.05 \text{ mg kg}^{-1}$ ) compared to that for peat fuels (13–69  $\text{mg kg}^{-1}$ ). Among all peat samples,  
504 the Alaskan peat fresh EF was the lowest EF ( $13.5 \pm 0.9 \text{ mg kg}^{-1}$ ), whereas Moscow peat fresh  
505 emissions yielded the highest EF ( $69 \pm 4.4 \text{ mg kg}^{-1}$ ). The difference in total aromatic acid emissions  
506 can be attributed to the variation in the lignin content of the fuels and burning conditions (Simoneit,  
507 2002).

508

509



511  
 512 Figure 2e. EFs of resin acids in both particulate phase (solid bars, filter samples) and gas-phase  
 513 (open bars, XAD samples) from fresh biomass-burning emissions for six different biomass types.  
 514 As in prior cases, we did not burn fuels in replicates, and SD were calculated based on replicate  
 515 analysis of similar fuels (with same experimental conditions) from our previous campaigns  
 516 (Yatavelli et al., 2017) and SD varies from 9.7–15% for resin acids

517 We quantitatively analyzed combustion emissions for isomers in six resin acids (Table S1). The  
518 most abundant resin acid (78% of total resin acid emission) is dehydroabietic acid (C<sub>20</sub>) that does  
519 not have isomers. The preponderance of this acid over other resin acids in emissions from oak and  
520 pine biomass burning was reported by Simoneit et al. (1993). We found that dehydroabietic acid  
521 (C<sub>20</sub>) content in fresh emissions is 15–30 times higher in fuels from high-latitude peatlands than in  
522 those of tropical origin. For example, the EF for dehydroabietic acid in fresh Alaskan peat  
523 emissions is 92.2±14 mg kg<sup>-1</sup> (Fig. 2e), whereas the same in fresh Malaysian peat emissions is  
524 3.44±0.5 mg kg<sup>-1</sup> (Fig. 2e). Resin acids are supposed to be found mostly in particulate phase based  
525 on their MW and functional groups (Asher et al., 2002; Karlberg et al., 1988; Pankow and Asher,  
526 2008), confirmed by our results (80–100% in particulate phase) with the exception of Malaysian  
527 peat emissions where 56.6% abundance of dehydroabietic acid was found in gas phase. Although  
528 a distinct peak of dehydroabietic acid was observed at the desired retention time for this sample  
529 during GC-MS analysis, we believe this result can be attributed to some unknown interference  
530 from our analysis procedure.

531  
532 The EF<sub>group</sub> for seven resin acids are presented in Fig. 3e. High EF<sub>group</sub> was observed for Alaskan  
533 (117±15 mg kg<sup>-1</sup>), Pskov (89±12 mg kg<sup>-1</sup>), and Moscow (59±7.7 mg kg<sup>-1</sup>) peats representing mid  
534 latitude and arctic peats. Resin acids (e.g., pimaric acid) are biosynthesized mainly by conifers  
535 (gymnosperms) in temperate regions. In previous work, Iinuma et al. (2007) gave a range of resin  
536 acids EFs from 0 to 110 mg kg<sup>-1</sup>, in agreement with our results. Very low resin acids EFs were  
537 found for peat from tropical regions (e.g., 4 mg kg<sup>-1</sup> for Malaysian peat fresh samples). As  
538 deciduous trees in tropical zones are not prolific resin and mucilage (gum) producers,  
539 compositional data on smoke from such sources should not be expected to show moderate  
540 concentrations of resin acids. This is supported by earlier work by Iinuma et al. (2007), where resin  
541 acids were not even detectable for emissions from Indonesian peat combustion.

### 542 543 *3.1.5 Levoglucosan*

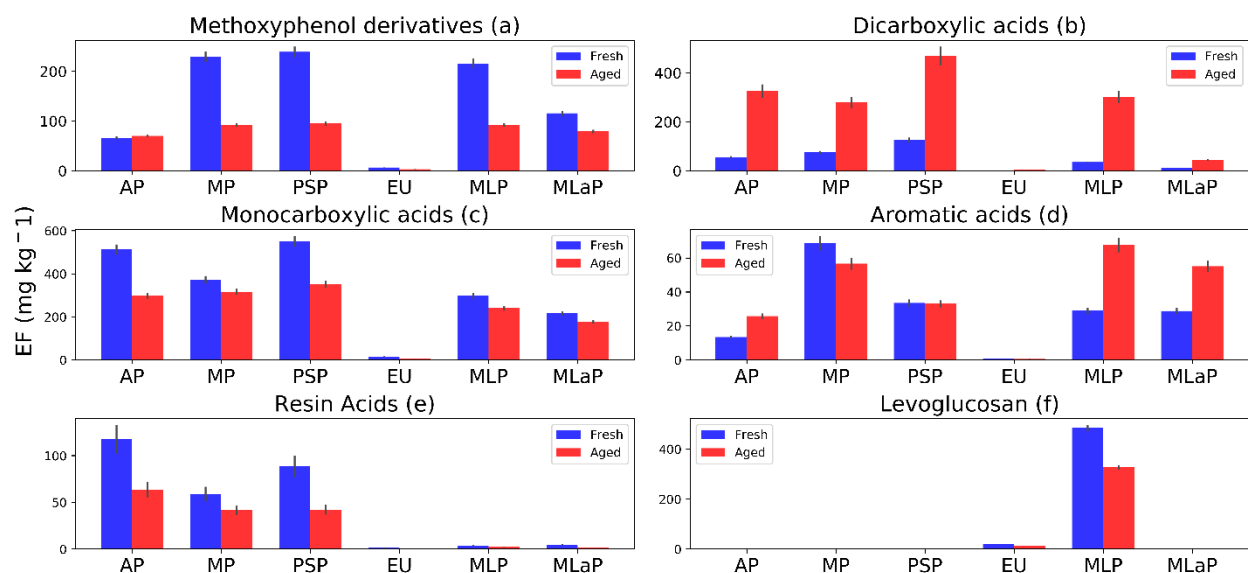
544 Levoglucosan can be found mostly in particulate phase (Simoneit, 2002). We report levoglucosan  
545 EFs from our analysis of the quartz filter using the IC-PAD technique (no gas phase EFs reported).



546 The EFs of levoglucosan (Fig. 3f) were found to be  $20.9 \pm 0.68 \text{ mg kg}^{-1}$  and  $485 \pm 11.8 \text{ mg kg}^{-1}$  for  
 547 Eucalyptus and Malaysian peat, respectively, and their carbon content is approximately 1.8% and  
 548 2.5 % of the total organic carbon mass characterized by the thermo-optical technique. Fine et al.  
 549 (2002) reported 9% to 16% contribution of levoglucosan to total OC from residential wood  
 550 combustion, a relatively higher percentage than values obtained in our study. Anhydrosugars (e.g.,  
 551 levoglucosan and its isomers) are found in great abundance and have been widely used as a BB  
 552 tracer because of their atmospheric stability, as summarized by Bhattarai et al. (2019). We found  
 553 that levoglucosan constituted 36% and 51% of GC-MS characterized polar (listed in our method)  
 554 organic aerosol mass for eucalyptus and Malaysian peat, respectively, which also is consistent with  
 555 the previous BB literature assembled in the recent review article by Bhattarai et al. (2019).

### 557 3.2. Emission factors of total (gas + particle) organic compounds of six chemical groups and 558 their changes upon OFR oxidations

559  
 560 Here we describe changes in the  $EF_{\text{group}}$  followed by OFR oxidation for all six chemical groups.  
 561 Levoglucosan and the most abundant resin acid, dehydroabietic acid also are reported in this  
 562 section.



563  
 564 **Figure 3.** Fuel-based emission factors (EFs) of organic compounds assigned to six chemical  
 565 groups for six different fuels: Alaskan peat (AP), Moscow peat (MP), Pskov peat (PSP),

566 Eucalyptus (EU), Malaysian peat (MLP), Malaysian agricultural peat (MLaP). EFs are presented  
567 as a sum of gas- and particle-phase species mass measured in fresh and OFR-aged BB emissions  
568 in units of  $\text{mg kg}^{-1}$  (mass of emissions per fuel mass combusted). We did not burn fuels in  
569 replicates, and standard deviations (SD) of all chemical groups were calculated based on replicate  
570 analysis of similar fuels (with same experimental conditions) from our previous campaign based  
571 on the data reported by Yatavelli et al. (2017).

572

### 573 *3.2.1. Methoxyphenol derivatives after OFR oxidation (Fig. 3a)*

574 Methoxyphenols can undergo gas-phase oxidation reactions via either aromatic ring  
575 fragmentation/opening to form short-chain ketones, acids, esters, and double bonds in conjugations  
576 with all functional groups or further hydroxylation of aromatic rings to form multiple substituted  
577 aromatic compounds (Yee et al., 2013). In either case, a decrease in methoxyphenols after  
578 oxidation was expected. In our study, a decrease in methoxyphenol's  $\text{EF}_{\text{group}}$  with OFR oxidations  
579 were observed for all fuels (e.g., for Pskov peat from  $239 \pm 11 \text{ mg kg}^{-1}$  to  $95 \pm 4 \text{ mg kg}^{-1}$ ) except for  
580 Alaskan peat, where an insignificant increase from  $66 \pm 3 \text{ mg kg}^{-1}$  to  $70 \pm 3 \text{ mg kg}^{-1}$  after the OFR  
581 oxidation was observed.

582

### 583 *3.2.2. Dicarboxylic acid group after OFR oxidation (Fig. 3b)*

584 A significant increase (2.5–8.5 times) in the  $\text{EF}_{\text{group}}$  of dicarboxylic acids was observed for OFR-  
585 aged samples. For example, the  $\text{EF}_{\text{group}}$  of dicarboxylic acids increased from  $35 \pm 3 \text{ mg kg}^{-1}$  to  
586  $301 \pm 25 \text{ mg kg}^{-1}$  for Malaysian peat and from  $56 \pm 5 \text{ mg kg}^{-1}$  to  $326 \pm 27 \text{ mg kg}^{-1}$  for Alaskan peat.  
587 Oxidation of aerosols potentially produces more oxygenated functional groups (Jimenez et al.,  
588 2009), demonstrated by an increase in O:C ratios (from 0.45 to 0.65) in recent laboratory oxidation  
589 of BB emissions by Bertrand et al. (2018), where TAG-AMS was used to identify the fate of  
590 organic compounds. In this work, however, the number of identifiable compounds with highly  
591 functional groups is constrained by the elution technique used in the TAG method. Our results on  
592 the fate of BB organic aerosols with 18 dicarboxylic acids can provide better mechanistic  
593 understanding about the processes inside OFR.

594

595 3.2.3. Monocarboxylic acid group after OFR oxidation (Fig. 3c)

596 We observed a decrease in monocarboxylic acids  $EF_{\text{group}}$  from OFR aging for all fuels. For  
597 example, the  $EF_{\text{group}}$  for monocarboxylic acids from Alaskan peat combustion decreased from  
598  $514 \pm 23 \text{ mg kg}^{-1}$  (fresh) to  $298 \pm 14 \text{ mg kg}^{-1}$  (aged). A relatively small decrease compared to Alaskan  
599 peat was observed for Malaysian agricultural peat (from  $216 \pm 10 \text{ mg kg}^{-1}$  [fresh] to  $179 \pm 8 \text{ mg kg}^{-1}$   
600 [aged]) and Malaysian peat (from  $298 \pm 14 \text{ mg kg}^{-1}$  [fresh] to  $240 \pm 11 \text{ mg kg}^{-1}$  [aged]) too. This is  
601 probably because of the formation of low MW monocarboxylic acids (e.g., hexanoic acids;  
602  $MW=116 \text{ g mol}^{-1}$ ) after OFR oxidation demonstrated in Fig. 4c and Table S2c and will be  
603 discussed further in section 3.3. Monocarboxylic acids can be oxidized in the atmosphere  
604 (Charbouillot et al., 2012), leading to the formation of dicarboxylic acids from  $C_2$  to  $C_6$  (Ervens et  
605 al., 2004). This is consistent with our results (Figs. 3b, 3c, Table S2b) Moreover, monocarboxylic  
606 acids, during their atmospheric transformations, can produce a potential precursor for formation  
607 of high MW compounds, such as Humic Like Substance (HULIS) (Carlton et al., 2007; Tan et al.,  
608 2012).

609

610 3.2.4. Aromatic acid group after OFR oxidation (Fig. 3d)

611 Levels of aromatic acids from peat burning increased for Alaskan peat, Malaysian peat, and  
612 Malaysian agricultural peat (e.g., from  $29 \pm 2 \text{ mg kg}^{-1}$  to  $68 \pm 4 \text{ mg kg}^{-1}$  for Malaysian peat) by OFR  
613 aging (Fig. 3e, Table S2e). This increase could be from oxidation of phenols and methoxyphenols  
614 in the OFR chamber (Akagi et al., 2011; Legrand et al., 2016). For eucalyptus, Moscow and Pskov  
615 peats it was an insignificantly small decrease (e.g., from  $69 \pm 4 \text{ mg kg}^{-1}$  to  $57 \pm 3 \text{ mg kg}^{-1}$  for  
616 Moscow peat and from  $34 \pm 2 \text{ mg kg}^{-1}$  to  $33 \pm 2 \text{ mg kg}^{-1}$  for Pskov peat). This small decrease in the  
617  $EF_{\text{group}}$  of monocarboxylic acids is insignificant. The oxidation processes occurring in the OFR are  
618 complex, especially in the case of multi-component BB emissions. The decrease observed for  
619 aromatic acids after the OFR may be attributed, however, to multiple generations of oxidation  
620 leading to the breaking of aromatic rings and formation of low MW organic compounds via  
621 fragmentation (Jimenez et al., 2009).

622

623

624 3.2.5. *Resin acids after OFR oxidation (Figs. 3d and 4e)*

625 Resin acids can be oxidized to corresponding oxo-acids (e.g., 7-oxodehydroabietic acid (Karlberg  
626 et al., 1988)), and they are considered to be stronger contact allergens than the resin acids  
627 themselves (Sadhra et al., 1998). Our data showed a small decrease in 7-oxodehydroabietic acid  
628 levels after the OFR (e.g., from  $8.2 \pm 0.8$  to  $4.8 \pm 0.5$  mg kg<sup>-1</sup> for Pskov peat). We noted a significant  
629 decrease in the EF<sub>group</sub> of resin acids from  $117 \pm 15$  mg kg<sup>-1</sup> (fresh) and  $63 \pm 8$  mg kg<sup>-1</sup> (aged) for  
630 Alaskan peat after OFR oxidation, mostly because of some individual compounds like  
631 dehydroabietic acid. Although resin acids are considered to be stable atmospheric tracers for  
632 biomass burning (Simoneit et al., 1993a), we observed a decrease in dehydroabietic acid (most  
633 abundant) EF after the OFR-oxidation of emissions from all fuels (Fig. S2b). For example, for  
634 Alaskan peat (Fig. S2b), the decrease was from  $92 \pm 14$  mg kg<sup>-1</sup> to  $57 \pm 8$  mg kg<sup>-1</sup> after OFR-  
635 oxidation. The fate of resin acids during OFR aging, however, was beyond the scope of this work  
636 and may be the subject of future investigations.

637

638 3.2.6. *Levoglucosan after OFR oxidation (Fig. 3f)*

639 Levoglucosan is one of the most popular tracers of BB emissions, since it has been considered a  
640 stable compound in the atmosphere (Oros et al., 2006; Simoneit, 2002; Simoneit et al., 1999).  
641 Several laboratory studies, however, have demonstrated degradation of levoglucosan in the  
642 presence of OH radicals (Hennigan et al., 2010). Here we observed a decrease of 30% in  
643 levoglucosan levels following OFR oxidation. For example, Malaysian peat decreased from  
644  $485 \pm 12$  mg kg<sup>-1</sup> to  $327 \pm 8$  mg kg<sup>-1</sup>. For eucalyptus, the decrease was from  $20 \pm 0.7$  mg kg<sup>-1</sup> to  $14 \pm 0.6$   
645 mg kg<sup>-1</sup>. This decrease also can be attributed to the degradation process during OH oxidation  
646 (Hoffmann et al., 2010). Levoglucosan oxidation should be studied more, so it can be adequately  
647 used as a tracer of BB emissions.

648

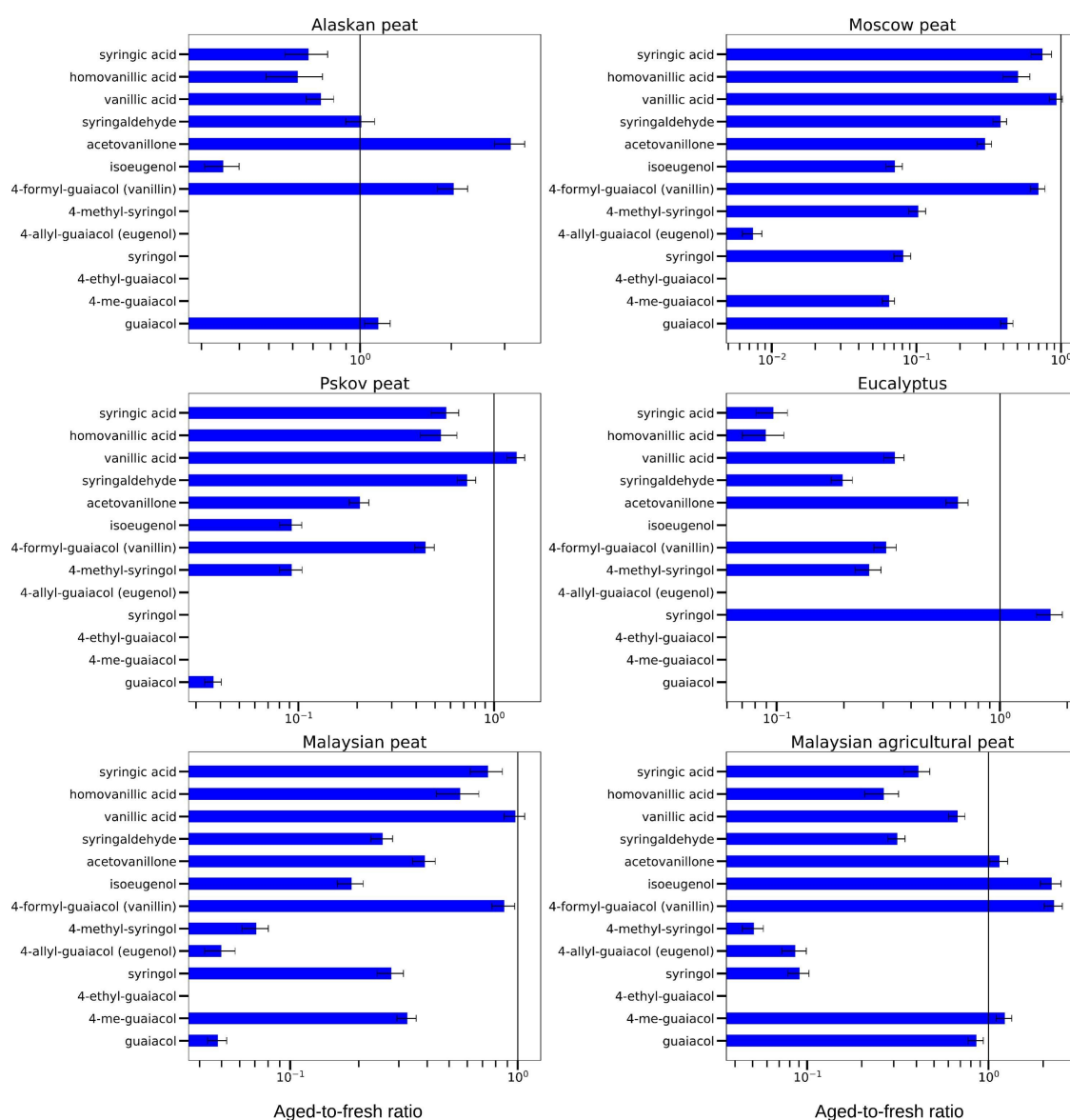
649 **3.3. Aged-to-fresh ratios of total (gas + particle) emission factors of individual organic**  
 650 **compounds assigned to six chemical groups and their changes upon OFR oxidation**

651 We computed aged-to-fresh ratios of individual compounds for all fuels. If the aged-to-fresh ratio  
 652 of one compound is greater than one, this implies that the compound is formed during OFR  
 653 oxidations; if the ratio is less than one, then the compound must have decomposed inside the OFR.

654

655 **3.3.1 Methoxyphenol Derivatives**

Methoxyphenol derivatives



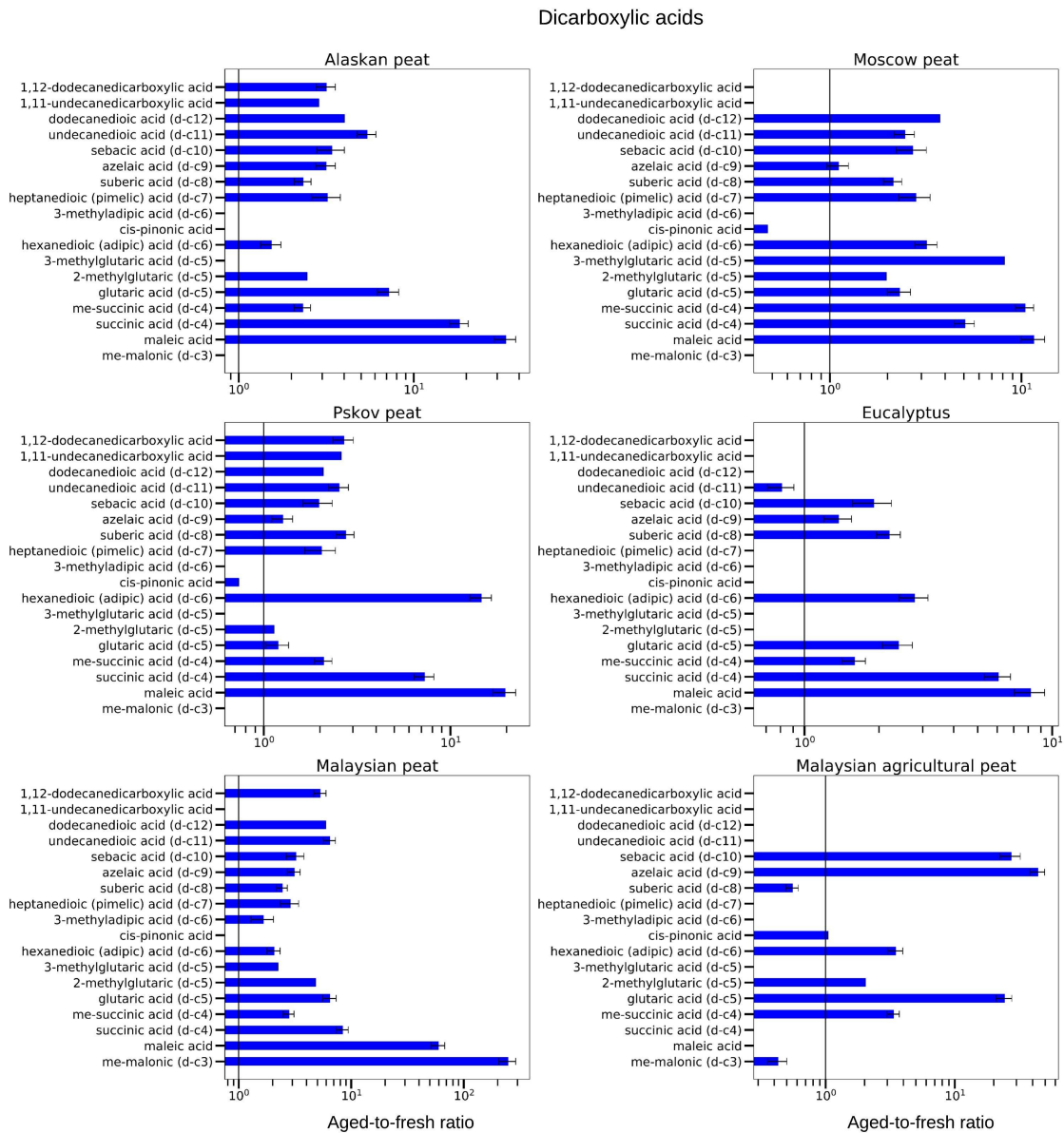
656

657 Figure 4a. Aged-to-fresh ratios of total (gas + particle) EFs for methoxyphenols from biomass  
658 burning emissions for six different biomass types presented in log scale. We did not burn fuels in  
659 replicates, and standard deviations (SD) were calculated based on replicate analysis of similar fuels  
660 (with same experimental conditions) from our previous campaigns. SD values derived from EFs  
661 were scaled to ratio.

662

663 Overall, we found that abundances for methoxyphenol derivatives rapidly decreased upon OFR-  
664 oxidation (Fig. 4a, Table S2a). Some compounds—vanillic acid, acetovanillone, and syringic  
665 acids— demonstrated both increasing and decreasing trends. For example, for Pskov peat, the  
666 aged-to-fresh ratio of guaiacol was  $0.04 \pm 0.01$  reflecting a significant decrease during OFR  
667 oxidation. For Pskov peat, we also observed a ratio less than one for vanillin ( $0.44 \pm 0.05$ ),  
668 indicating vanillin also decreased during OFR oxidation for the same fuel but not to the extent of  
669 guaiacol. At the same time and for the same fuel, a slight increase (aged-to-fresh ratio  $>1$ ) in  
670 vanillic acid was observed ( $1.30 \pm 0.13$ ) in the OFR-oxidized sample. This increase in vanillic acid  
671 concentration can be attributed to the oxidation of vanillin, one of the abundant methoxyphenol in  
672 the fresh emissions from Pskov peat (Fig. 4a, Table S2a). For combustion of other peats, vanillic  
673 acid concentrations also decreased (e.g., aged-to-fresh ratios were  $0.74 \pm 0.08$  and  $0.67 \pm 0.07$  for  
674 Alaskan peat and Malaysian agricultural peat, respectively). Acetovanillone increased by a factor  
675 of three during OFR oxidation for Alaskan peat and around 15 % for Malaysian agricultural peat  
676 (aged-to-fresh ratio  $1.15 \pm 0.13$ ), but the increase for Malaysian agricultural peat was not  
677 significant. For other fuels, acetovanillone decreased during the OFR oxidation. For example, for  
678 Moscow Peat, the aged-to-fresh ratio for acetovanillone was  $0.30 \pm 0.03$ . We still need to investigate  
679 the reason why both acetovanillone and vanillic acid increased for some fuels and decreased for  
680 others. The reduction of acetovanillone and vanillic acid was because of a photo-chemical  
681 decomposition process in the OFR with formation of lower MW products, such as succinic acid  
682 and maleic acid (Schnitzler and Abbatt, 2018).

683



685

686 Figure 4b. Aged-to-fresh ratios of total (gas + particle) EFs for dicarboxylic acids from biomass  
 687 burning emissions for six different biomass types presented in log scale. We did not burn fuels in  
 688 replicates, and SD were calculated based on replicate analysis of similar fuels (with same  
 689 experimental conditions) from our previous campaigns. SD values derived from EFs were scaled  
 690 to ratio.

691

692 In the case of dicarboxylic acids, we observed 2–20 times increase in EFs, but the degree of  
693 enhancement of low MW dicarboxylic acids EFs was higher than for high MW dicarboxylic acids  
694 EFs. For example, a 20-fold increase in maleic acid, a low MW dicarboxylic acid (MW= 116.07  
695 g mol<sup>-1</sup>), was observed during OFR oxidation of Pskov peat emissions (aged-to-fresh ratio =  
696 19.6±2.8), whereas 1,11-undecanedicarboxylic acid, a high MW dicarboxylic acid (MW = 244.33  
697 g mol<sup>-1</sup>), EF increased 2.6 times (aged-to-fresh ratio = 2.60±0.01) for the same fuel. Similarly, the  
698 concentration of succinic acid, a low MW dicarboxylic acid (MW= 118.09 g mol<sup>-1</sup>), increased  
699 almost by five times after OFR oxidation (aged-to-fresh ratio = 5.07±0.62), whereas that of  
700 undecanedioic acid, a high MW dicarboxylic acid (MW = 230.30 g mol<sup>-1</sup>), increased 2.5 times  
701 (aged-to-fresh ratio = 2.46±0.30) for Moscow peat. This trend was in accord with results from  
702 ambient observations after BB events (Cao et al., 2017; Kawamura and Bikkina, 2016).

703

704

705

706

707

708

709

710

711

712

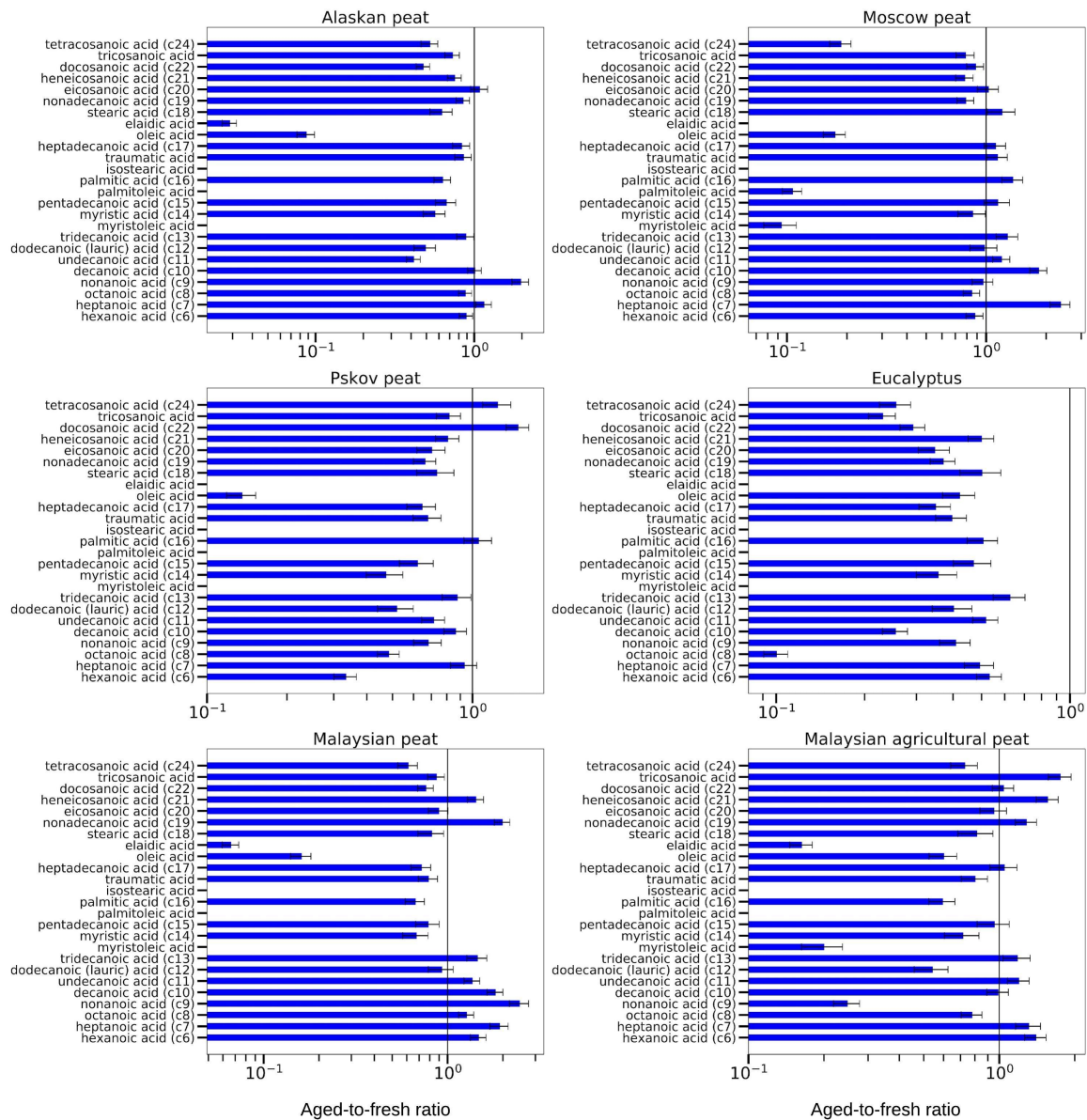
713

714

715



Monocarboxylic acids



717  
 718 **Figure 4c.** Aged-to-fresh ratios of total (gas + particle) EFs for monocarboxylic acids from  
 719 biomass burning emissions for six different biomass types presented in log scale. We did not burn  
 720 fuels in replicates, and SD were calculated based on replicate analysis of similar fuels (with same  
 721 experimental conditions) from our previous campaigns. SD values derived from EFs were scaled  
 722 to ratio.

723

724 Our analysis of OFR-aged samples showed that concentrations of monocarboxylic acids with  
725 different MWs changed during OFR oxidation, but the changes varied from one fuel to another.  
726 For example, the EF of hexanoic acid ( $C_6$ ) was reduced for Eucalyptus (aged-to-fresh ratio =  
727  $0.5\pm 0.05$ ) and fuels from other high-latitude peatlands like Alaskan (aged-to-fresh ratio =  
728  $0.89\pm 0.09$ ), Moscow (aged-to-fresh ratio =  $0.88\pm 0.09$ ) and Pskov peat (aged-to-fresh ratio =  
729  $0.33\pm 0.03$ ). The reduction of hexadecenoic acid was insignificant for Alaskan and Moscow peat.  
730 The peats from tropical regions showed exactly the opposite change. Hexanoic acid increased for  
731 both Malaysian (aged-to-fresh ratio =  $1.47\pm 0.14$ ) and Malaysian agricultural peat (aged- to-fresh  
732 ratio =  $1.40\pm 0.14$ ). We observed a similar trend for heptanoic acid ( $C_7$ ) during OFR oxidation. The  
733 tropical peats clearly demonstrated increases (for example, aged-to-fresh ratio =  $1.92\pm 0.22$  for  
734 Malaysian peat) in heptanoic acid concentration. For Moscow peat, even though hexanoic acid  
735 concentrations were insignificantly decreased, heptanoic acid concentrations increased  
736 significantly (aged-to-fresh ratio =  $2.37\pm 0.27$ ). This contrast between changes in hexanoic and  
737 heptanoic acid can be explained by a decrease in CPI indices during OFR oxidations (for example,  
738 from 2.78 to 1.7 for Malaysian peat). The reduction of CPI indices indicated that during oxidation  
739 more monocarboxylic acids with odd carbon numbers were formed than monocarboxylic acids  
740 with even carbon numbers. The abundance of hexadecenoic acid ( $C_{16}$ ) was reduced during OFR  
741 oxidation for all fuels (for example, aged-to-fresh ratio =  $0.63\pm 0.08$  for Alaskan peat) except for  
742 Moscow and Pskov peat aged-to-fresh ratio =  $1.05\pm 0.13$  for peat), and we believe this small  
743 increase is insignificant. Similarly, tetracosanoic acid ( $C_{20}$ ) was reduced for all fuels (for example,  
744 aged-to-fresh ratio =  $0.61\pm 0.07$  for Malaysian peat) except for Pskov peat (aged-to-fresh ratio =  
745  $1.24\pm 0.15$ ). The small increase in tetracosanoic acid ( $C_{20}$ ) concentration was again insignificant.  
746 Even though our results indicated the possibility of fragmentation of high MW monocarboxylic  
747 acids and formation of low MW monocarboxylic acids, this was because of the complexity of the  
748 OFR oxidation environment. We are not able to hypothesize what is the main reactive mechanism.

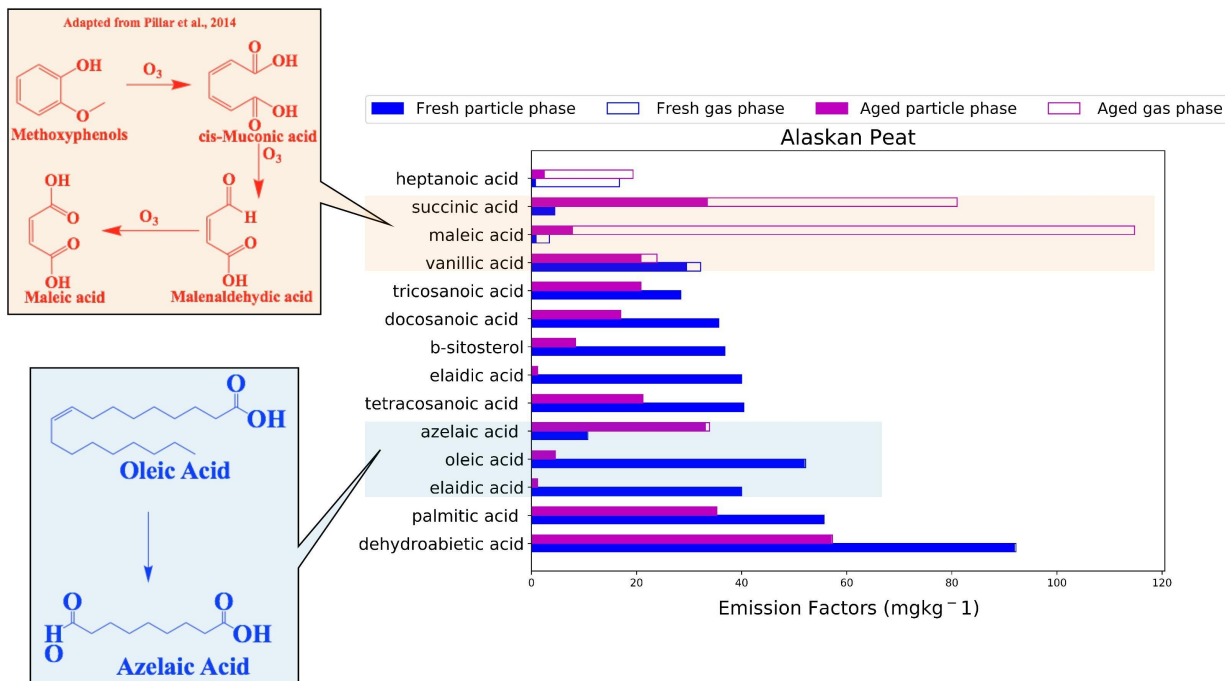
749

750

751

752

753 **3.4. Most Contributing Compounds**



754

755

756 **Figure 5.** Emission factors (EF) of top contributing organic compounds assigned to Alaskan peat.

757 Top 10 contributing compounds were selected from both fresh and aged emissions based on EF  
 758 values. Since fresh and aged samples do not have the same set of compounds after the selection,  
 759 we included the top 10 compounds for both fresh and aged emissions. Hence, the number of top  
 760 contributing compounds varies from one fuel to another. Solid bars of each type represent a  
 761 chemical group from particulate emission of BB fuels and open bars of the same color represent  
 762 gas phase BB emissions.

763

764 We have identified top contributing compounds for both fresh and aged BB emissions of each fuel  
 765 to understand how emissions vary from one fuel to another. The top 10 compounds for fresh and  
 766 aged emission were different, and we merged the top 10 compounds from fresh and aged emissions  
 767 resulting in different numbers of total top compounds for different fuels. Here we discuss Alaskan  
 768 peat emissions in their particulate phase (with solid bars) and gas phase (with open bars) as an  
 769 example, while the remaining results are given in the SM (Figs S3 and S4). It is clear that the top

770 compounds vary between fuels, likely because of both different chemical nature of these fuels and  
771 nature of combustion.

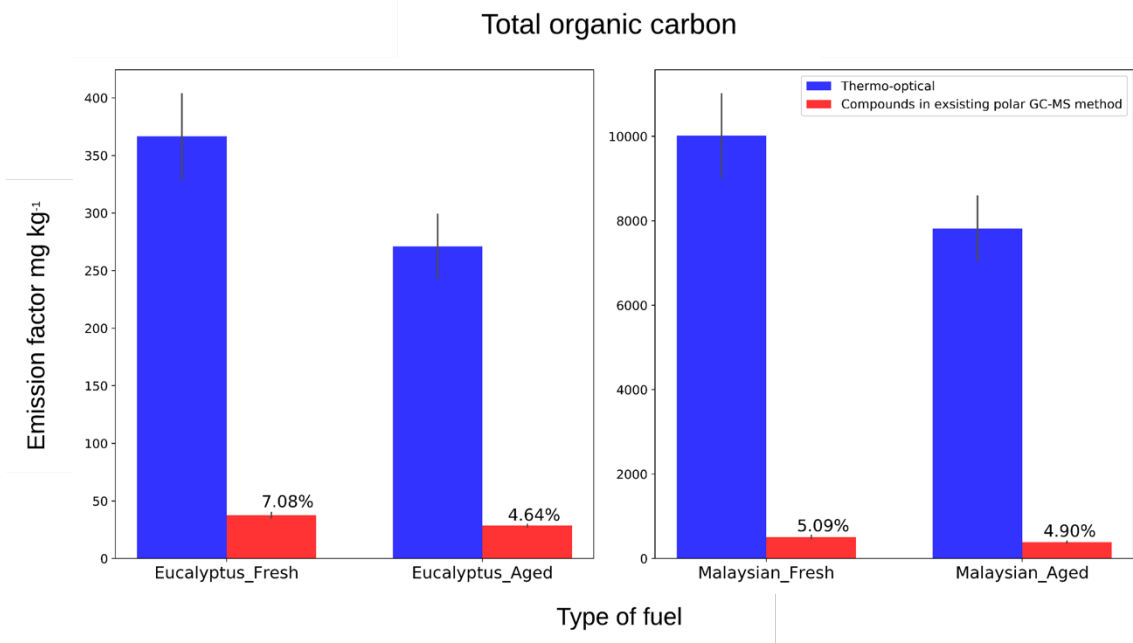
772

773 Dehydroabietic acid, a resin acid, is the compound with the highest EF ( $92.2 \text{ mg kg}^{-1}$ ) for fresh  
774 combustion emissions from Alaskan peat. Moncarboxylic acids including palmitic acid ( $\text{EF} = 55.7$   
775  $\text{mg kg}^{-1}$ ), tetracosanoic acid ( $\text{EF} = 40.35 \text{ mg kg}^{-1}$ ), and docosanoic acid ( $\text{EF} = 35.38 \text{ mg kg}^{-1}$ ) were  
776 also found in high abundance in fresh emissions from the combustion of this fuel. The high  
777 contributions of  $\beta$ -sitosterol ( $\text{EF} = 36.84 \text{ mg kg}^{-1}$ ) and alkenoic acids (e.g., oleic acid  $\text{EF} = 52.1$   
778  $\text{mg kg}^{-1}$ ) to emissions are unique to Alaskan peat. All the compounds described above are found  
779 in particulate phase. After the OFR-oxidation, both dehydroabietic acid and  $\beta$ -sitosterol, considered  
780 to be potential markers for biomass burning emissions (Simoneit et al., 1993b), decreased from  
781  $91.9 \text{ mg kg}^{-1}$  to  $57.2 \text{ mg kg}^{-1}$  and  $36.8 \text{ mg kg}^{-1}$  to  $8.38 \text{ mg kg}^{-1}$  in particulate phase, respectively.  
782 This reduction in EF because of OFR oxidation for both dehydroabietic acid and  $\beta$ -sitosterol must  
783 be considered when using these compounds as biomass-burning markers. We observed the  
784 formation of low MW organic compounds, particularly in gas phase, from OFR oxidation. For  
785 example, the EF of heptanoic acid increased from  $2.42 \text{ mg kg}^{-1}$  to  $16.9 \text{ mg kg}^{-1}$  and that of maleic  
786 acid increased from  $7.8 \text{ mg kg}^{-1}$  to  $107 \text{ mg kg}^{-1}$  in the gas phase because of OFR oxidation. Such  
787 a significant increase in the EF of maleic acid can be explained by the aqueous phase oxidation of  
788 methoxyphenols (El Zein et al., 2015) in the presence of ozone. We found that the oxidation inside  
789 the chamber was happening under dry conditions and understand that the reactions of organic  
790 compounds with OH radicals inside the OFR chamber will prevail over reactions with ozone. As  
791 we had our ozone scrubbers placed after sampling media (Fig. 1) to prevent the pumps and online  
792 instruments from ozone-induced damage, we suspect that the maleic acid was not formed inside  
793 the OFR chamber but rather by potential oxidation of organic compounds on filters with relatively  
794 longer exposure of ozone (40–60 min for smoldering combustion). Succinic acid EFs increased in  
795 both the gas phase (from  $0.0 \text{ mg kg}^{-1}$  to  $47.5 \text{ mg kg}^{-1}$ ) and the particulate phase (from  $4.43 \text{ mg kg}^{-1}$   
796 to  $33.5 \text{ mg kg}^{-1}$ ). Azelaic acid EFs showed mainly an increase in the particulate phase (from  $10.5$   
797  $\text{mg kg}^{-1}$  to  $33.1 \text{ mg kg}^{-1}$ ), and we think that this was because of the oxidation of oleic and eladic  
798 acid during OFR oxidation.

799

800

801 **3.5 Contribution of polar fraction to total organic carbon**  
802



803  
804 **Figure 6.** Contribution of GC-MS characterized polar compound carbon mass to total thermo-  
805 optical organic carbon mass. The y-axis shows the total carbon mass with dimensions of mass per  
806 mass. The error bars represent analytical uncertainties of the methods. For the thermo-optical  
807 method, uncertainties are the standard deviation of results from multiple punches on the same filter  
808 and for the GC-MS method, uncertainties were computed by taking the square root of sum of the  
809 squares of individual analytical uncertainties of all compounds included.

810  
811 For Figure 6, we calculated the carbon content of total GC-MS characterized mass of identified  
812 polar organic compounds and compared results with the total OC mass characterized by the  
813 thermo-optical technique to estimate the contribution of polar compounds. The OC emissions were  
814 higher for smoldering combustion ( $10,209 \pm 5 \text{ mg kg}^{-1}$  for Malaysian peat fresh emissions) than  
815 for flaming combustion ( $366.5 \pm 7 \text{ mg kg}^{-1}$  for eucalyptus fresh emissions) samples, similar to the  
816 observation of flaming and smoldering combustion by Akagi et al. (2011). Total OC emissions  
817 are highly dependent on the type of fuel. For example, the fuel-based OC emission factor for rice  
818 crop residue burning is  $1960 \text{ mg kg}^{-1}$  (Cao et al., 2008), whereas burning of corn and conifer forest

819 yields emission factors of  $\sim 1457 \text{ mg kg}^{-1}$  (Andreae and Rosenfeld, 2008) and  $\sim 7800 \text{ mg kg}^{-1}$   
820 (Akagi et al., 2011), respectively. Figure 6 shows that the 84 identified polar compounds in our  
821 study constituted 4.5% to 7% of total OC mass for both fresh and aged emissions. From Indonesian  
822 peat combustion emissions, Jayarathne et al. (2018) were able to identify polar compounds that  
823 constituted 5.446% of total organic carbon mass. In recent work, based on both a field campaign  
824 with prescribed burning and laboratory investigations, Jen et al. (2019) quantified a fraction (10–  
825 65%) of only identified compounds (not a fraction of total mass) by the use of the 2D-GC-MS  
826 technique. In our work, we identified only up to 7% (Fig. 6) of the total particle phase OC, and  
827 further analysis of unidentified compounds is needed to improve understanding of atmospheric  
828 chemistry of BB emissions.

829

830

#### 831 **4. Summary and conclusions**

832 In this study, we chemically characterized the polar fraction of biomass-burning aerosols from  
833 laboratory combustion of six different globally and regionally important fuels—five of them  
834 representing smoldering and one of them representing flaming combustion. Our objective was to  
835 understand how emissions of the polar compounds (e.g., methoxyphenols) varied from one fuel to  
836 another during these combustion experiments and what are the relative distribution of these polar  
837 compounds in gas and particulate phase. We also identified the fates of these polar compounds  
838 following laboratory oxidation/aging (OFR aging). Resin acids were found mostly in emissions  
839 from combustion of peats from high latitude regions but not in emissions of tropical peatlands  
840 (e.g.,  $EF_{\text{group}} = 117 \pm 15 \text{ mg kg}^{-1}$  for Alaskan peat and  $EF_{\text{group}} = 4.0 \pm 0.5 \text{ mg kg}^{-1}$  for Malaysian peat).  
841 Similarly, monocarboxylic acids were found in higher abundance in emissions from high latitude  
842 peatlands compared to tropical peatland emissions (e.g.,  $EF_{\text{group}} = 505 \pm 36 \text{ mg kg}^{-1}$  for Alaskan peat  
843 and  $EF_{\text{group}} = 212 \pm 15 \text{ mg kg}^{-1}$  for Malaysian agricultural peat). The presence of both guaiacol and  
844 syringol moieties in all fuels indicated a part of the biomass, considered as representative of a  
845 particular geographical region, is deciduous for all fuels. Low MW compounds are mostly found  
846 in gas phase (e.g., guaiacol found in gas phase 82–100%), whereas high MW (e.g., monocarboxylic  
847 acids [ $>C_{16}$ ] more than 98% for all fuels) and highly oxygenated compounds (e.g., syringic acid  
848 and acetovanillone 65–100% in particulate phase) are found in particulate phase with high

849 abundance. Monocarboxylic acids (1.2–3 times) and methoxyphenols (1.5–2.5 times) decreased  
850 after OFR oxidation, whereas dicarboxylic acids increased by 3–9 times followed by OFR  
851 oxidation. Relatively low MW hexanoic acid increased for both Malaysian (aged-to-fresh ratio =  
852 1.47±0.14) and Malaysian agricultural peat (aged- to-fresh ratio = 1.40±0.14), whereas high MW  
853 tetracosanoic acid (C<sub>20</sub>) was reduced for all fuel increases (e.g., aged-to-fresh ratio = 0.61±0.07  
854 for Malaysian peat). This indicated fragmentation occurring inside the OFR chamber. With relative  
855 distribution of the top 10–15 compounds from Alaskan peat, we were able to identify  
856 transformation of unsaturated fatty acids (e.g., oleic acid) to dicarboxylic acids (e.g., azelaic acid).  
857 We identified only up to 7% of the total particle phase OC and further analysis of unidentified  
858 compounds with GC-MS full scan is needed for better understanding of atmospheric chemistry of  
859 BB emissions.

860

861

862 **Data availability.** Data can be provided upon request: <andrey.khlystov@dri.edu>.

863

864 **Author contributions.** DS, VS, and AK designed experiments. DS and CB performed sample,  
865 data collection, and extraction. DS performed derivatization, GC-MS analysis, summarized data,  
866 and wrote the paper. AW provided biomass fuels. VS, AK, and HM provided input on  
867 interpretation of results. VS, HM, and AK revised the manuscript.

868

869 **Competing interests.** The authors declare that they have no conflict of interest.

870

871 **Acknowledgements.** This research was supported by the National Science Foundation (NSF)  
872 under grant numbers AGS-1544425 and AGS-1408241, NASA ROSES under grant number  
873 NNX15AI48G, and internal funding from DRI. The authors would like to thank Anna Tsibar  
874 (Moscow State Lomonosov University, Moscow, Russia) for providing peat fuels from Russia.  
875 We acknowledge Benjamin Nault (CIRES, UC Boulder) and Andrew Lambe (Aerodyne) for their  
876 insightful discussion leading to identification of a potential artifact in our experimental set up  
877 associated with high maleic acid formation. The authors also thank Rodger Kreidberg for revising  
878 the manuscript.

879

880 REFERENCES

881 Akagi, S. K., Yokelson, R. J., Wiedinmyer, C., Alvarado, M. J., Reid, J. S., Karl, T., Crounse, J.  
882 D. and Wennberg, P. O.: Emission factors for open and domestic biomass burning for use in  
883 atmospheric models, *Atmos. Chem. Phys.*, 11(9), 4039–4072, doi:10.5194/acp-11-4039-2011,  
884 2011.

885 Alvarado, M. J., Lonsdale, C. R., Yokelson, R. J., Akagi, S. K., Coe, H., Craven, J. S., Fischer, E.  
886 V., McMeeking, G. R., Seinfeld, J. H., Soni, T., Taylor, J. W., Weise, D. R. and Wold, C. E.:  
887 Investigating the links between ozone and organic aerosol chemistry in a biomass burning plume  
888 from a prescribed fire in California chaparral, *Atmos. Chem. Phys.*, 15(12), 6667–6688,  
889 doi:10.5194/acp-15-6667-2015, 2015.

890 Andreae, M. O. and P. Merlet: Emission of trace gases and aerosols from biomass burning,  
891 *Global Biogeochem. Cycles*, 15(4), 955–966, doi:10.1029/2000GB001382, 2001.

892 Andreae, M. O. and Rosenfeld, D.: Aerosol-cloud-precipitation interactions. Part 1. The nature  
893 and sources of cloud-active aerosols, *Earth-Science Rev.*, 89(1–2), 13–41,  
894 doi:10.1016/j.earscirev.2008.03.001, 2008.

895 Arbex, M. A., Martins, L. C., Carvalho De Oliveira, R., Pereira, A. A., Arbex, F. F., Eduardo, J.,  
896 Cançado, D., Hilário, P., Saldiva, N., Luís, A. and Braga, F.: Air pollution from biomass burning  
897 and asthma hospital admissions in a sugar cane plantation area in Brazil, *J Epidemiol Community*  
898 *Heal.*, 61, 395–400, doi:10.1136/jech.2005.044743, 2007.

899 Asher, W. E., Pankow, J. F., Erdakos, G. B. and Seinfeld, J. H.: Estimating the vapor pressures of  
900 multi-functional oxygen-containing organic compounds using group contribution methods,  
901 *Atmos. Environ.*, 36(9), 1483–1498, doi:10.1016/S1352-2310(01)00564-7, 2002.

902 Bertrand, A., Stefenelli, G., Jen, C. N., Pieber, S. M., Bruns, E. A., Ni, H., Temime-Roussel, B.,  
903 Slowik, J. G., Goldstein, A. H., Haddad, I. El, Baltensperger, U., Prévôt, A. S. H., Wortham, H.  
904 and Marchand, N.: Evolution of the chemical fingerprint of biomass burning organic aerosol  
905 during aging, *Atmos. Chem. Phys.*, 18(10), 7607–7624, doi:10.5194/acp-18-7607-2018, 2018.

906 Bhattarai, C., Samburova, V., Sengupta, D., Iaukea-Lum, M., Watts, A. C., Moosmüller, H. and  
907 Khlystov, A. Y.: Physical and chemical characterization of aerosol in fresh and aged emissions  
908 from open combustion of biomass fuels, *Aerosol Sci. Technol.*, 52(11), 1266–1282,



909 doi:10.1080/02786826.2018.1498585, 2018.

910 Bhattarai, H., Saikawa, E., Wan, X., Zhu, H., Ram, K., Gao, S., Kang, S., Zhang, Q., Zhang, Y.,  
911 Wu, G., Wang, X., Kawamura, K., Fu, P. and Cong, Z.: Levoglucosan as a tracer of biomass  
912 burning: Recent progress and perspectives, *Atmos. Res.*, 220(September 2018), 20–33,  
913 doi:10.1016/j.atmosres.2019.01.004, 2019a.

914 Bhattarai, H., Saikawa, E., Wan, X., Zhu, H., Ram, K., Gao, S., Kang, S., Zhang, Q., Zhang, Y.,  
915 Wu, G., Wang, X., Kawamura, K., Fu, P. and Cong, Z.: Levoglucosan as a tracer of biomass  
916 burning: Recent progress and perspectives, *Atmos. Res.*, 220(September 2018), 20–33,  
917 doi:10.1016/j.atmosres.2019.01.004, 2019b.

918 Bonvalot, L., Tuna, T., Fagault, Y., Jaffrezo, J. L., Jacob, V., Chevrier, F. and Bard, E.: Estimating  
919 contributions from biomass burning, fossil fuel combustion, and biogenic carbon to carbonaceous  
920 aerosols in the Valley of Chamoni: A dual approach based on radiocarbon and levoglucosan,  
921 *Atmos. Chem. Phys.*, 16(21), 13753–13772, doi:10.5194/acp-16-13753-2016, 2016.

922 Cao, F., Zhang, S. C., Kawamura, K., Liu, X., Yang, C., Xu, Z., Fan, M., Zhang, W., Bao, M.,  
923 Chang, Y., Song, W., Liu, S., Lee, X., Li, J., Zhang, G. and Zhang, Y. L.: Chemical characteristics  
924 of dicarboxylic acids and related organic compounds in PM<sub>2.5</sub> during biomass-burning and non-  
925 biomass-burning seasons at a rural site of Northeast China, *Environ. Pollut.*, 231, 654–662,  
926 doi:10.1016/j.envpol.2017.08.045, 2017.

927 Cao, G., Zhang, X., Gong, S. and Zheng, F.: Investigation on emission factors of particulate matter  
928 and gaseous pollutants from crop residue burning, *J. Environ. Sci.*, 20(1), 50–55,  
929 doi:10.1016/S1001-0742(08)60007-8, 2008.

930 Carlton, A. G., Turpin, B. J., Altieri, K. E., Seitzinger, S., Reff, A., Lim, H. J. and Ervens, B.:  
931 Atmospheric oxalic acid and SOA production from glyoxal: Results of aqueous photooxidation  
932 experiments, *Atmos. Environ.*, 41(35), 7588–7602, doi:10.1016/j.atmosenv.2007.05.035, 2007.

933 Chakrabarty, R. K., Gyawali, M., Yatavelli, R. L. N., Pandey, A., Watts, A. C., Knue, J., Chen, L.  
934 W. A., Pattison, R. R., Tsbart, A., Samburova, V. and Moosmüller, H.: Brown carbon aerosols  
935 from burning of boreal peatlands: Microphysical properties, emission factors, and implications for  
936 direct radiative forcing, *Atmos. Chem. Phys.*, 16(5), 3033–3040, doi:10.5194/acp-16-3033-2016,  
937 2016.

938 Charbouillot, T., Gorini, S., Voyard, G., Parazols, M., Brigante, M., Deguillaume, L., Delort, A.  
939 M. and Mailhot, G.: Mechanism of carboxylic acid photooxidation in atmospheric aqueous phase:  
940 Formation, fate and reactivity, *Atmos. Environ.*, 56, 1–8, doi:10.1016/j.atmosenv.2012.03.079,  
941 2012.

942 Chen, J., Li, C., Ristovski, Z., Milic, A., Gu, Y., Islam, M. S., Wang, S., Hao, J., Zhang, H., He,  
943 C., Guo, H., Fu, H., Miljevic, B., Morawska, L., Thai, P., LAM, Y. F., Pereira, G., Ding, A.,  
944 Huang, X. and Dumka, U. C.: A review of biomass burning: Emissions and impacts on air quality,  
945 health and climate in China, *Sci. Total Environ.*, 579, 1000–1034,  
946 doi:10.1016/j.scitotenv.2016.11.025, 2017.

947 Chow, J. C. and Watson, J. G.: Enhanced Ion Chromatographic Speciation of Water-Soluble PM  
948 2.5 to Improve Aerosol Source Apportionment, *Aerosol Sci. Eng.*, 1(1), 7–24,  
949 doi:10.1007/s41810-017-0002-4, 2017.

950 Chow, J. C., Watson, J. G., Pritchett, L. C., Pierson, W. R., Frazier, C. A. and Purcell, R. G.: The  
951 DRI thermal optical reflectance carbon analysis system - description, evaluation and applications  
952 in United-States air quality studies, *Atmos. Environ. Part a-General Top.*, 27(8), 1185–1201, 1993.

953 Chow, J. C., Watson, J. G., Chen, L. W. A., Arnott, W. P., Moosmüller, H. and Fung, K.:  
954 Equivalence of elemental carbon by thermal/optical reflectance and transmittance with different  
955 temperature protocols, *Environ. Sci. Technol.*, 38(16), 4414–4422, doi:10.1021/es034936u, 2004.

956 Decker, Z. C. J., Zarzana, K. J., Coggon, M., Min, K. E., Pollack, I., Ryerson, T. B., Peischl, J.,  
957 Edwards, P., Dubé, W. P., Markovic, M. Z., Roberts, J. M., Veres, P. R., Graus, M., Warneke, C.,  
958 De Gouw, J., Hatch, L. E., Barsanti, K. C. and Brown, S. S.: Nighttime Chemical Transformation  
959 in Biomass Burning Plumes: A Box Model Analysis Initialized with Aircraft Observations,  
960 *Environ. Sci. Technol.*, 53(5), 2529–2538, doi:10.1021/acs.est.8b05359, 2019.

961 Dills, R. L., Paulsen, M., Ahmad, J., Kalman, D. A., Elias, F. N. and Simpson, C. D.: Evaluation  
962 of urinary methoxyphenols as biomarkers of woodsmoke exposure, *Environ. Sci. Technol.*, 40(7),  
963 2163–2170, doi:10.1021/es051886f, 2006.

964 Ervens, B., Feingold, G., Frost, G. J. and Kreidenweis, S. M.: A modeling of study of aqueous  
965 production of dicarboxylic acids: 1. Chemical pathways and speciated organic mass production, *J.*  
966 *Geophys. Res. D Atmos.*, 109(15), 1–20, doi:10.1029/2003JD004387, 2004.

967 Fang, M., Zheng, M., Wang, F., To, K. L., Jaafar, A. B. and Tong, S. L.: The solvent-extractable  
968 organic compounds in the Indonesia biomass burning aerosols - Characterization studies, *Atmos.*  
969 *Environ.*, 33(5), 783–795, doi:10.1016/S1352-2310(98)00210-6, 1999.

970 Fine, P. M., Cass, G. R. and Simoneit, B. R. T.: Organic compounds in biomass smoke from  
971 residential wood combustion: Emissions characterization at a continental scale, *J. Geophys. Res.*  
972 *Atmos.*, 107(21), 1–9, doi:10.1029/2001JD000661, 2002.

973 Finlayson-Pitts, B. J. and Pitts Jr, J. N.: *Chemistry of the upper and lower atmosphere: theory,*  
974 *experiments, and applications*, Elsevier., 1999.

975 Fortenberry, C. F., Walker, M. J., Zhang, Y., Mitroo, D., Brune, W. H. and Williams, B. J.: Bulk  
976 and molecular-level characterization of laboratory-aged biomass burning organic aerosol from oak  
977 leaf and heartwood fuels, *Atmos. Chem. Phys.*, 18(3), 2199–2224, doi:10.5194/acp-18-2199-2018,  
978 2018.

979 Freimuth, E. J., Diefendorf, A. F., Lowell, T. V. and Wiles, G. C.: Sedimentary n-alkanes and n-  
980 alkanoic acids in a temperate bog are biased toward woody plants, *Org. Geochem.*, 128, 94–107,  
981 doi:10.1016/j.orggeochem.2019.01.006, 2019.

982 Goldstein, A. H. and Galbally, I. E.: Known and unexplored organic constituents in the earth's  
983 atmosphere, *Environ. Sci. Technol.*, 41(5), 1514–1521, doi:10.1021/es072476p, 2007.

984 Goodrick, S. L. and Stanturf, J. A.: Evaluating Potential Changes in Fire Risk from Eucalyptus  
985 Plantings in the Southern United States , *Int. J. For. Res.*, 2012, 1–9, doi:10.1155/2012/680246,  
986 2012.

987 Graham, B., Mayol-Bracero, O. L., Guyon, P., Roberts, G. C., Decesari, S., Facchini, M. C.,  
988 Artaxo, P., Maenhaut, W., Köll, P. and Andreae, M. O.: Water-soluble organic compounds in  
989 biomass burning aerosols over Amazonia 1. Characterization by NMR and GC-MS, *J. Geophys.*  
990 *Res. Atmos.*, 107(20), doi:10.1029/2001JD000336, 2002.

991 Grieshop, A. P., Donahue, N. M. and Robinson, A. L.: Laboratory investigation of photochemical  
992 oxidation of organic aerosol from wood fires 2: analysis of aerosol mass spectrometer data, *Atmos.*  
993 *Chem. Phys.*, 9, 2227–2240, doi:10.5194/acp-9-2227-2009, 2009.

994 Harden, J., Trumbore, S., Stocks, B., Hirsch, A., Gower, S., O'neill, K. and Kasischke, E.: The  
995 role of fire in the boreal carbon budget, *Glob. Chang. Biol.*, 6, 174–184, doi:10.1046/j.1365-

996 2486.2000.06019.x, 2000.

997 Hawthorne, S. B., Krieger, M. S., Miller, D. J. and Mathiason, M. B.: Collection and Quantitation  
998 of Methoxylated Phenol Tracers for Atmospheric Pollution from Residential Wood Stoves,  
999 *Environ. Sci. Technol.*, 23(4), 470–475, doi:10.1021/es00181a013, 1989.

1000 Hedges, J. I. and Ertel, J. R.: Characterization of Lignin by Gas Capillary Chromatography of  
1001 Cupric Oxide Oxidation Products, *Anal. Chem.*, 54(2), 174–178, doi:10.1021/ac00239a007, 1982.

1002 Hennigan, C. J., Sullivan, A. P., Collett, J. L. and Robinson, A. L.: Levoglucosan stability in  
1003 biomass burning particles exposed to hydroxyl radicals, *Geophys. Res. Lett.*, 37(9), 2–5,  
1004 doi:10.1029/2010GL043088, 2010.

1005 Hills, W.E.; Brown, A. G. .: *Eucalypts for wood production.*, CSIRO., Canberra., 1978.

1006 Hoffmann, D., Tilgner, A., Inuma, Y. and Herrmann, H.: Atmospheric stability of levoglucosan:  
1007 A detailed laboratory and modeling study, *Environ. Sci. Technol.*, 44(2), 694–699,  
1008 doi:10.1021/es902476f, 2010.

1009 Inuma, Y., Brüggemann, E., Gnauk, T., Müller, K., Andreae, M. O., Helas, G., Parmar, R. and  
1010 Herrmann, H.: Source characterization of biomass burning particles: The combustion of selected  
1011 European conifers, African hardwood, savanna grass, and German and Indonesian peat, *J.*  
1012 *Geophys. Res. Atmos.*, 112(8), doi:10.1029/2006JD007120, 2007.

1013 Jayarathne, T., Stockwell, C. E., Gilbert, A. A., Daugherty, K., Cochrane, M. A., Ryan, K. C.,  
1014 Putra, E. I., Saharjo, B. H., Nurhayati, A. D., Albar, I., Yokelson, R. J. and Stone, E. A.: Chemical  
1015 characterization of fine particulate matter emitted by peat fires in Central Kalimantan, Indonesia,  
1016 during the 2015 El Niño, *Atmos. Chem. Phys.*, 18(4), 2585–2600, doi:10.5194/acp-18-2585-2018,  
1017 2018.

1018 Jen, C. N., Hatch, L. E., Selimovic, V., Yokelson, R. J., Weber, R., Fernandez, A. E., Kreisberg,  
1019 N. M., Barsanti, K. C. and Goldstein, A. H.: Speciated and total emission factors of particulate  
1020 organics from burning western US wildland fuels and their dependence on combustion efficiency,  
1021 *Atmos. Chem. Phys.*, 19(2), 1013–1026, doi:10.5194/acp-19-1013-2019, 2019.

1022 Jimenez, J. L., Canagaratna, M. R., Donahue, N. M., Prevot, A. S. H., Zhang, Q., Kroll, J. H.,  
1023 DeCarlo, P. F., Allan, J. D., Coe, H., Ng, N. L., Aiken, A. C., Docherty, K. S., Ulbrich, I. M.,  
1024 Grieshop, A. P., Robinson, A. L., Duplissy, J., Smith, J. D., Wilson, K. R., Lanz, V. A., Hueglin,

1025 C., Sun, Y. L., Tian, J., Laaksonen, A., Raatikainen, T., Rautiainen, J., Vaattovaara, P., Ehn, M.,  
1026 Kulmala, M., Tomlinson, J. M., Collins, D. R., Cubison, M. J., Dunlea, E. J., Huffman, J. A.,  
1027 Onasch, T. B., Alfarra, M. R., Williams, P. I., Bower, K., Kondo, Y., Schneider, J., Drewnick, F.,  
1028 Borrmann, S., Weimer, S., Demerjian, K., Salcedo, D., Cottrell, L., Griffin, R., Takami, A.,  
1029 Miyoshi, T., Hatakeyama, S., Shimono, A., Sun, J. Y., Zhang, Y. M., Dzepina, K., Kimmel, J. R.,  
1030 Sueper, D., Jayne, J. T., Herndon, S. C., Trimborn, A. M., Williams, L. R., Wood, E. C.,  
1031 Middlebrook, A. M., Kolb, C. E., Baltensperger, U. and Worsnop, D. R.: Evolution of organic  
1032 aerosols in the atmosphere, *Science* (80-. ), 326(5959), 1525–1529, doi:10.1126/science.1180353,  
1033 2009.

1034 Jung, J., Lyu, Y., Lee, M., Hwang, T., Lee, S. and Oh, S.: Impact of Siberian forest fires on the  
1035 atmosphere over the Korean Peninsula during summer 2014, *Atmos. Chem. Phys.*, 16(11), 6757–  
1036 6770, doi:10.5194/acp-16-6757-2016, 2016.

1037 Karlberg, A.-T., Boman, A., Hacksell, U., Jacobsson, S. and Nilsson, J. L. G.: Contact allergy to  
1038 dehydroabietic acid derivatives isolated from Portuguese colophony, *Contact Dermatitis*, 19(3),  
1039 166–174, 1988.

1040 Kawamura, K. and Bikkina, S.: A review of dicarboxylic acids and related compounds in  
1041 atmospheric aerosols: Molecular distributions, sources and transformation, *Atmos. Res.*, 170, 140–  
1042 160, doi:10.1016/j.atmosres.2015.11.018, 2016.

1043 Kessler, S. H., Smith, J. D., Che, D. L., Worsnop, D. R., Wilson, K. R. and Kroll, J. H.: Chemical  
1044 Sinks of Organic Aerosol: Kinetics and Products of the Heterogeneous Oxidation of Erythritol and  
1045 Levoglucosan, *Environ. Sci. Technol.*, 44(18), 7005–7010, doi:10.1021/es101465m, 2010.

1046 Kundu, S., Kawamura, K., Andreae, T. W., Hoffer, A. and Andreae, M. O.: Molecular distributions  
1047 of dicarboxylic acids, ketocarboxylic acids and  $\alpha$ -dicarbonyls in biomass burning aerosols:  
1048 implications for photochemical production and degradation in smoke layers, *Atmos. Chem. Phys.*,  
1049 10(5), 2209–2225, doi:10.5194/acp-10-2209-2010, 2010.

1050 Legrand, M., McConnell, J., Fischer, H., Wolff, E. W., Preunkert, S., Arienzo, M., Chellman, N.,  
1051 Leuenberger, D., Maselli, O., Place, P., Sigl, M., Schüpbach, S. and Flannigan, M.: Boreal fire  
1052 records in Northern Hemisphere ice cores: A review, *Clim. Past*, 12(10), 2033–2059,  
1053 doi:10.5194/cp-12-2033-2016, 2016.

1054 Li, R., Palm, B. B., Ortega, A. M., Hlywiak, J., Hu, W., Peng, Z., Day, D. A., Knote, C., Brune,  
1055 W. H., de Gouw, J. A. and Jimenez, J. L.: Modeling the Radical Chemistry in an Oxidation Flow  
1056 Reactor: Radical Formation and Recycling, Sensitivities, and the OH Exposure Estimation  
1057 Equation., *J. Phys. Chem. A*, 119(19), 4418–4432, doi:10.1021/jp509534k, 2015.

1058 Liu, X., Huey, L. G., Yokelson, R. J., Selimovic, V., Simpson, I. J., Müller, M., Jimenez, J. L.,  
1059 Campuzano-Jost, P., Beyersdorf, A. J., Blake, D. R., Butterfield, Z., Choi, Y., Crounse, J. D., Day,  
1060 D. A., Diskin, G. S., Dubey, M. K., Fortner, E., Hanisco, T. F., Hu, W., King, L. E., Kleinman, L.,  
1061 Meinardi, S., Mikoviny, T., Onasch, T. B., Palm, B. B., Peischl, J., Pollack, I. B., Ryerson, T. B.,  
1062 Sachse, G. W., Sedlacek, A. J., Shilling, J. E., Springston, S., St. Clair, J. M., Tanner, D. J., Teng,  
1063 A. P., Wennberg, P. O., Wisthaler, A. and Wolfe, G. M.: Airborne measurements of western U.S.  
1064 wildfire emissions: Comparison with prescribed burning and air quality implications, *J. Geophys.*  
1065 *Res.*, 122(11), 6108–6129, doi:10.1002/2016JD026315, 2017.

1066 Maenhaut, W., Vermeylen, R., Claeys, M., Vercauteren, J. and Roekens, E.: Sources of the PM10  
1067 aerosol in Flanders, Belgium, and re-assessment of the contribution from wood burning, *Sci. Total*  
1068 *Environ.*, 562, 550–560, doi:10.1016/j.scitotenv.2016.04.074, 2016.

1069 Mazzoleni, L. R., Zielinska, B. and Moosmüller, H.: Emissions of levoglucosan, methoxy phenols,  
1070 and organic acids from prescribed burns, laboratory combustion of wildland fuels, and residential  
1071 wood combustion, *Environ. Sci. Technol.*, 41(7), 2115–2122, doi:10.1021/es061702c, 2007.

1072 Müller-Tautges, C., Eichler, A., Schwikowski, M., Pezzatti, G. B., Conedera, M. and Hoffmann,  
1073 T.: Historic records of organic compounds from a high Alpine glacier: Influences of biomass  
1074 burning, anthropogenic emissions, and dust transport, *Atmos. Chem. Phys.*, 16(2), 1029–1043,  
1075 doi:10.5194/acp-16-1029-2016, 2016.

1076 Net, S., Alvarez, E. G., Gligorovski, S. and Wortham, H.: Heterogeneous reactions of ozone with  
1077 methoxyphenols, in presence and absence of light, *Atmos. Environ.*, 45(18), 3007–3014,  
1078 doi:10.1016/j.atmosenv.2011.03.026, 2011.

1079 Oros, D. R. and Simoneit, B. R. T.: Identification and emission factors of molecular tracers in  
1080 organic aerosols from biomass burning Part 1. Temperate climate conifers, *Appl. Geochemistry*,  
1081 16(13), 1513–1544, doi:https://doi.org/10.1016/S0883-2927(01)00021-X, 2001a.

1082 Oros, D. R. and Simoneit, B. R. T.: Identification and emission factors of molecular tracers in

1083 organic aerosols from biomass burning Part 2. Deciduous trees, *Appl. Geochemistry*, 16(13),  
1084 1545–1565, doi:[https://doi.org/10.1016/S0883-2927\(01\)00022-1](https://doi.org/10.1016/S0883-2927(01)00022-1), 2001b.

1085 Oros, D. R., Abas, M. R. bin, Omar, N. Y. M. J., Rahman, N. A. and Simoneit, B. R. T.:  
1086 Identification and emission factors of molecular tracers in organic aerosols from biomass burning:  
1087 Part 3. Grasses, *Appl. Geochemistry*, 21(6), 919–940, doi:10.1016/j.apgeochem.2006.01.008,  
1088 2006.

1089 Ortega, A. M., Day, D. A., Cubison, M. J., Brune, W. H., Bon, D., de Gouw, J. A. and Jimenez, J.  
1090 L.: Secondary organic aerosol formation and primary organic aerosol oxidation from biomass-  
1091 burning smoke in a flow reactor during FLAME-3, *Atmos. Chem. Phys.*, 13(22), 11551–11571,  
1092 doi:10.5194/acp-13-11551-2013, 2013.

1093 Pankow, J. F. and Asher, W. E.: SIMPOL.1: A simple group contribution method for predicting  
1094 vapor pressures and enthalpies of vaporization of multifunctional organic compounds, *Atmos.*  
1095 *Chem. Phys.*, 8(10), 2773–2796, doi:10.5194/acp-8-2773-2008, 2008.

1096 Pardo, M., Li, C., He, Q., Levin-Zaidman, S., Tsoory, M., Yu, Q., Wang, X. and Rudich, Y.:  
1097 Mechanisms of lung toxicity induced by biomass burning aerosols, *Part. Fibre Toxicol.*, 17(1), 1–  
1098 15, doi:10.1186/s12989-020-0337-x, 2020.

1099 Park, R. J., Jacob, D. J. and Logan, J. A.: Fire and biofuel contributions to annual mean aerosol  
1100 mass concentrations in the United States, *Atmos. Environ.*, 41(35), 7389–7400,  
1101 doi:10.1016/j.atmosenv.2007.05.061, 2007.

1102 Pavagadhi, S., Betha, R., Venkatesan, S., Balasubramanian, R. and Hande, M. P.: Physicochemical  
1103 and toxicological characteristics of urban aerosols during a recent Indonesian biomass burning  
1104 episode, *Environ. Sci. Pollut. Res.*, 20(4), 2569–2578, doi:10.1007/s11356-012-1157-9, 2013.

1105 Penner, J. E., Ghan, S. J. and Walton, J. J.: The role of biomass burning in the budget and cycle of  
1106 carbonaceous soot aerosols and their climate impact. [online] Available from:  
1107 [https://inis.iaea.org/search/search.aspx?orig\\_q=RN:23067068](https://inis.iaea.org/search/search.aspx?orig_q=RN:23067068) (Accessed 8 September 2019),  
1108 1991.

1109 Ramanathan, V. and Carmichael, G.: Global and regional climate changes due to black carbon,  
1110 *Nat. Geosci.*, 1(4), 221–227, doi:10.1038/ngeo156, 2008.

1111 Regalado, J., Pérez-Padilla, R., Sansores, R., Ramirez, J. I. P., Brauer, M., Paré, P. and Vedal, S.:

1112 The effect of biomass burning on respiratory symptoms and lung function in rural Mexican  
1113 women, *Am. J. Respir. Crit. Care Med.*, 174(8), 901–905, doi:10.1164/rccm.200503-479OC,  
1114 2006.

1115 Rinehart, L. R., Fujita, E. M., Chow, J. C., Magliano, K. and Zielinska, B.: Spatial distribution of  
1116 PM<sub>2.5</sub> associated organic compounds in central California, *Atmos. Environ.*, 40(2), 290–303,  
1117 doi:10.1016/j.atmosenv.2005.09.035, 2006.

1118 Sadhra, S., Foulds, I. S. and Gray, C. N.: Oxidation of resin acids in colophony (rosin) and its  
1119 implications for patch testing, *Contact Dermatitis*, 39(2), 58–63, doi:10.1111/j.1600-  
1120 0536.1998.tb05833.x, 1998.

1121 Samburova, V., Hallar, A. G., Mazzoleni, L. R., Saranjampour, P., Lowenthal, D., Kohl, S. D. and  
1122 Zielinska, B.: Composition of water-soluble organic carbon in non-urban atmospheric aerosol  
1123 collected at the Storm Peak Laboratory, *Environ. Chem.*, 10(5), 370–380  
1124 <https://doi.org/10.1071/EN13079>, 2013.

1125 Samburova, V., Connolly, J., Gyawali, M., Yatavelli, R. L. N., Watts, A. C., Chakrabarty, R. K.,  
1126 Zielinska, B., Moosmüller, H. and Khlystov, A.: Polycyclic aromatic hydrocarbons in biomass-  
1127 burning emissions and their contribution to light absorption and aerosol toxicity, *Sci. Total*  
1128 *Environ.*, 568, 391–401, doi:10.1016/j.scitotenv.2016.06.026, 2016.

1129 Sarkanen, K. V and Ludwig, C. H.: *Lignins: occurrence, formation, structure and reactions*, Wiley-  
1130 interscience, New York., 1971.

1131 Schauer, J. J., Kleeman, M. J., Cass, G. R. and Simoneit, B. R. T.: Measurement of emissions from  
1132 air pollution sources. 3. C<sub>1</sub>-C<sub>29</sub> organic compounds from fireplace combustion of wood, *Environ.*  
1133 *Sci. Technol.*, 35(9), 1716–1728, doi:10.1021/es001331e, 2001.

1134 Schmidl, C., Marr, I. L., Caseiro, A., Kotianová, P., Berner, A., Bauer, H., Kasper-Giebl, A. and  
1135 Puxbaum, H.: Chemical characterisation of fine particle emissions from wood stove combustion  
1136 of common woods growing in mid-European Alpine regions, *Atmos. Environ.*, 42(1), 126–141,  
1137 doi:10.1016/j.atmosenv.2007.09.028, 2008a.

1138 Schmidl, C., Bauer, H., Dattler, A., Hitzenberger, R., Weissenboeck, G., Marr, I. L. and Puxbaum,  
1139 H.: Chemical characterisation of particle emissions from burning leaves, *Atmos. Environ.*, 42(40),  
1140 9070–9079, doi:10.1016/j.atmosenv.2008.09.010, 2008b.



1141 Schnitzler, E. G. and Abbatt, J. P. D.: Heterogeneous OH oxidation of secondary brown carbon  
1142 aerosol, *Atmos. Chem. Phys.*, 18(19), 14539–14553, doi:10.5194/acp-18-14539-2018, 2018.

1143 Sengupta, D., Samburova, V., Bhattarai, C., Kirillova, E., Mazzoleni, L., Iaukea-Lum, M., Watts,  
1144 A., Moosmüller, H. and Khlystov, A.: Light absorption by polar and non-polar aerosol compounds  
1145 from laboratory biomass combustion, *Atmos. Chem. Phys.*, 18(15), 10849–10867,  
1146 doi:10.5194/acp-18-10849-2018, 2018.

1147 Sigsgaard, T., Forsberg, B., Annesi-Maesano, I., Blomberg, A., Bølling, A., Boman, C., Bønløkke,  
1148 J., Brauer, M., Bruce, N., Héroux, M. E., Hirvonen, M. R., Kelly, F., Künzli, N., Lundbäck, B.,  
1149 Moshhammer, H., Noonan, C., Pagels, J., Sallsten, G., Sculier, J. P. and Brunekreef, B.: Health  
1150 impacts of anthropogenic biomass burning in the developed world, *Eur. Respir. J.*, 46(6), 1577–  
1151 1588, doi:10.1183/13993003.01865-2014, 2015.

1152 Simoneit, B. R. T.: Biomass burning — a review of organic tracers for smoke from incomplete  
1153 combustion, *Appl. Geochemistry*, 17(3), 129–162, doi:https://doi.org/10.1016/S0883-  
1154 2927(01)00061-0, 2002.

1155 Simoneit, B. R. T., Rogge, W. F., Mazurek, M. A., Standley, L. J., Hildemann, L. M. and Cass, G.  
1156 R.: Lignin pyrolysis products, lignans, and resin acids as specific tracers of plant classes in  
1157 emissions from biomass combustion, *Environ. Sci. Technol.*, 27(12), 2533–2541,  
1158 doi:10.1021/es00048a034, 1993.

1159 Simoneit, B. R. T., Schauer, J. J., Nolte, C. G., Oros, D. R., Elias, V. O., Fraser, M. P., Rogge, W.  
1160 F. and Cass, G. R.: Levoglucosan, a tracer for cellulose in biomass burning and atmospheric  
1161 particles, *Atmos. Environ.*, 33(2), 173–182, doi:10.1016/S1352-2310(98)00145-9, 1999.

1162 Simpson, C. D. and Naeher, L. P.: Biological monitoring of wood-smoke exposure, *Inhal. Toxicol.*,  
1163 22(2), 99–103, doi:10.3109/08958370903008862, 2010.

1164 Tan, Y., Lim, Y. B., Altieri, K. E., Seitzinger, S. P. and Turpin, B. J.: Mechanisms leading to  
1165 oligomers and SOA through aqueous photooxidation: Insights from OH radical oxidation of acetic  
1166 acid and methylglyoxal, *Atmos. Chem. Phys.*, 12(2), 801–813, doi:10.5194/acp-12-801-2012,  
1167 2012.

1168 Tian, J., Chow, J. C., Cao, J., Han, Y., Ni, H., Chen, L. A., Wang, X., Huang, R., Moosmüller, H.  
1169 and Watson, J. G.: A Biomass Combustion Chamber : Design , Evaluation , and a Case Study of

- 1170 Wheat Straw Combustion Emission Tests, , 2104–2114, doi:10.4209/aaqr.2015.03.0167, 2015.
- 1171 Turetsky, M. R., Benscoter, B., Page, S., Rein, G., Van Der Werf, G. R. and Watts, A.: Global  
1172 vulnerability of peatlands to fire and carbon loss, *Nat. Geosci.*, 8(1), 11–14,  
1173 doi:10.1038/ngeo2325, 2015.
- 1174 Wan, X., Kawamura, K., Ram, K., Kang, S., Loewen, M., Gao, S., Wu, G., Fu, P., Zhang, Y.,  
1175 Bhattarai, H. and Cong, Z.: Aromatic acids as biomass-burning tracers in atmospheric aerosols and  
1176 ice cores: A review, *Environ. Pollut.*, 247, 216–228, doi:10.1016/j.envpol.2019.01.028, 2019.
- 1177 Watts, A. C., Schmidt, C. A., McLaughlin, D. L. and Kaplan, D. A.: Hydrologic implications of  
1178 smoldering fires in wetland landscapes, *Freshw. Sci.*, 34(4), 1394–1405, doi:10.1086/683484,  
1179 2015.
- 1180 Yang, X. Y., Igarashi, K., Tang, N., Lin, J. M., Wang, W., Kameda, T., Toriba, A. and Hayakawa,  
1181 K.: Indirect- and direct-acting mutagenicity of diesel, coal and wood burning-derived particulates  
1182 and contribution of polycyclic aromatic hydrocarbons and nitropolycyclic aromatic hydrocarbons,  
1183 *Mutat. Res. - Genet. Toxicol. Environ. Mutagen.*, 695(1–2), 29–34,  
1184 doi:10.1016/j.mrgentox.2009.10.010, 2010.
- 1185 Yatavelli, R. L. N., Chen, L.-W. A., Knue, J., Samburova, V., Gyawali, M., Watts, A. C.,  
1186 Chakrabarty, R. K., Moosmüller, H., Hodzic, A., Wang, X., Zielinska, B., Chow, J. C. and Watson,  
1187 J. G.: Emissions and Partitioning of Intermediate-Volatility and Semi-Volatile Polar Organic  
1188 Compounds (I/SV-POCs) During Laboratory Combustion of Boreal and Sub-Tropical Peat,  
1189 *Aerosol Sci. Eng.*, 1(1), 25–32, doi:10.1007/s41810-017-0001-5, 2017.
- 1190 Yee, L. D., Kautzman, K. E., Loza, C. L., Schilling, K. A., Coggon, M. M., Chhabra, P. S., Chan,  
1191 M. N., Chan, A. W. H., Hersey, S. P., Crouse, J. D., Wennberg, P. O., Flagan, R. C. and Seinfeld,  
1192 J. H.: Secondary organic aerosol formation from biomass burning intermediates: Phenol and  
1193 methoxyphenols, *Atmos. Chem. Phys.*, 13(16), 8019–8043, doi:10.5194/acp-13-8019-2013, 2013.
- 1194 Yokelson, R. J., Bertschi, I. T., Christian, T. J., Hobbs, P. V., Ward, D. E. and Hao, W. M.: Trace  
1195 gas measurements in nascent, aged, and cloud-processed smoke from African savanna fires by  
1196 airborne Fourier transform infrared spectroscopy (AFTIR), *J. Geophys. Res. Atmos.*, 108(D13),  
1197 n/a-n/a, doi:10.1029/2002JD002322, 2003.
- 1198 El Zein, A., Coeur, C., Obeid, E., Lauraguais, A. and Fagniez, T.: Reaction Kinetics of Catechol

1199 (1,2-Benzenediol) and Guaiacol (2-Methoxyphenol) with Ozone, *J. Phys. Chem. A*, 119(26),  
1200 6759–6765, doi:10.1021/acs.jpca.5b00174, 2015.

1201 Zhu, Y., Yang, L., Chen, J., Kawamura, K., Sato, M., Tilgner, A., van Pinxteren, D., Chen, Y.,  
1202 Xue, L., Wang, X., Herrmann, H. and Wang, W.: Molecular distributions of dicarboxylic acids,  
1203 oxocarboxylic acids, and  $\alpha$ -dicarbonyls in PM<sub>2.5</sub> collected at Mt. Tai, in North China in 2014,  
1204 *Atmos. Chem. Phys.*, 1–31, doi:10.5194/acp-2017-1240, 2018.

1205

1206

1207